

Mutual Orbital Inclinations Between Cold Jupiters and Inner Super-Earths

KENTO MASUDA,^{1,2,*} JOSHUA N. WINN,¹ AND HAJIME KAWAHARA^{3,4}

¹*Department of Astrophysical Sciences, Princeton University, Princeton, NJ 08544, USA*

²*Institute for Advanced Study, Princeton, NJ 08540, USA*

³*Department of Earth and Planetary Science, The University of Tokyo, Tokyo 113-0033, Japan*

⁴*Research Center for the Early Universe, School of Science, The University of Tokyo, Tokyo 113-0033, Japan*

ABSTRACT

Previous analyses of Doppler and *Kepler* data have found that Sun-like stars hosting “cold Jupiters” (giant planets with $a \gtrsim 1$ AU) almost always host “inner super-Earths” ($1\text{--}4 R_{\oplus}$, $a \lesssim 1$ AU). Here, we attempt to determine the degree of alignment between the orbital planes of the cold Jupiters and the inner super-Earths. The key observational input is the fraction of *Kepler* stars with transiting super-Earths that also have transiting cold Jupiters. This fraction depends on both the probability for cold Jupiters to occur in such systems, and on the mutual orbital inclinations. Since the probability of occurrence has already been measured in Doppler surveys, we can use the data to constrain the dispersion of the mutual inclination distribution. We find $\sigma = 11.8_{-5.5}^{+12.7}$ deg (68% confidence) and $\sigma > 3.5$ deg (95% confidence), where σ is the scale parameter of the Rayleigh distribution. This suggests that planetary orbits in systems with cold Jupiters tend to be coplanar — although not quite as coplanar as those in the Solar System, which have a mean inclination from the invariable plane of 1.8 deg. We also find evidence that cold Jupiters have lower mutual inclinations relative to inner systems with higher transit multiplicity. This suggests a link between the dynamical excitation in the inner and outer systems. For example, perturbations from misaligned cold Jupiters may dynamically heat or destabilize systems of inner super-Earths.

Keywords: methods: data analysis — methods: statistical — techniques: photometric — techniques: spectroscopic — planets and satellites: dynamical evolution and stability

1. INTRODUCTION

Doppler surveys showed long ago that wide-orbiting giant planets have a broader eccentricity distribution than the planets in the Solar System (e.g., [Butler et al. 2006](#)). Since planetary systems are thought to form in a “dynamically cold” state, with nearly circular and coplanar orbits, high eccentricities are usually interpreted as evidence for post-formation perturbations due to planet–planet interactions or the influence of a neighboring star (e.g., [Rasio & Ford 1996](#); [Weidenschilling & Marzari 1996](#); [Holman et al. 1997](#)). If these systems have been dynamically heated, one might also expect the mutual inclinations between planetary orbits to have a broader range than the dispersion of a few degrees seen in the Solar System. This prediction has been difficult

to test because mutual inclinations are more difficult to measure than eccentricities.

The Doppler method only allows mutual inclinations to be measured directly when planet–planet gravitational interactions are unusually strong (see, e.g., [Laughlin et al. 2002](#)). In those few special cases, all of which involve multiple giant planets, the mutual inclinations have been found to be $\lesssim 10^\circ$. The Doppler and astrometric techniques have also been used together to demonstrate a 30° inclination between two giant planets in the ν And system ([McArthur et al. 2010](#)). Less directly, [Dawson & Chiang \(2014\)](#) found evidence for $\approx 40^\circ$ mutual inclinations in systems featuring a “warm Jupiter” (semi-major axis $a = 0.1$ to 1 AU) and a “balmy Jupiter” ($a > 1$ AU), based on the observed tendency for the directions of periapses of the two orbits to be nearly orthogonal.

The transit method can also provide direct constraints on mutual inclinations in special cases, as well as indirect constraints based on observed statistical patterns.

Corresponding author: Kento Masuda
kmasuda@ias.edu

* NASA Sagan Fellow

Direct constraints have been obtained from analyses of the observed variations in transit times and durations in strongly interacting multi-planet systems (see, e.g., Sanchis-Ojeda et al. 2012; Nesvorný et al. 2012), and a unique example of a planet–planet eclipse (Hirano et al. 2012). In these cases the mutual inclinations were found to be smaller than about 10° , with the exception of Kepler-108, in which two Saturn-mass planets have orbits inclined by 24_{-8}^{+11} degrees (Mills & Fabrycky 2017). A less direct method is based on the comparison of transit impact parameters (Fabrycky et al. 2014). This method has been used to show that mutual inclinations are typically smaller than a few degrees among the *Kepler* compact multi-planet systems — except when the innermost planet has an exceptionally small orbit (with an orbital distance less than 5–6 stellar radii) in which case the inclination dispersion is $\gtrsim 7^\circ$ (Dai et al. 2018).

A different indirect technique is based on the observed transit multiplicity function: the relative numbers of stars with 1, 2, 3, \dots , N detected transiting planets. All else being equal, flatter planetary systems are more likely to be observed as systems with higher transit multiplicity. However, the transit multiplicity function depends not only on mutual inclinations but also on the multiplicity function without regard to transits, i.e., the probability that 1, 2, 3, \dots , N planets exist at all. For example, the detection of a single transiting planet might mean only one planet exists, or that the planet is part of a system of multiple planets on misaligned orbits. Zhu et al. (2018) broke this degeneracy by analyzing both the transit multiplicity function and the occurrence of transit timing variations (TTVs), which are less sensitive to mutual inclinations. They found a model that successfully explains the observed transit multiplicity function of *Kepler* planetary systems, including the relatively large number of stars with a single detected transiting planet (Lissauer et al. 2011; Fang & Margot 2012; Tremaine & Dong 2012; Johansen et al. 2012). In their model, the mutual inclination dispersion is assumed to decrease with multiplicity: in systems with 3 or more planets the dispersion is found to be $\lesssim 5^\circ$, while for two-planet systems the dispersion is found to be $\sim 10^\circ$.

The degeneracy between multiplicity and mutual inclinations can also be broken by combining the results of transit and Doppler surveys (Tremaine & Dong 2012; Figueira et al. 2012), which is the technique employed in this paper. Specifically, we attempted to determine the distribution of mutual inclinations between two types of planets which sometimes occur together in the same system: the typical *Kepler* planets with sizes between

1 and $4 R_\oplus$ and orbital distances less than 1 AU, which we call “inner super-Earths” or simply “SEs”; and giant planets on orbits wider than 1 AU, which we call “cold Jupiters” or “CJs”.¹

We chose to focus on SEs and CJs because the necessary information has become available only recently, and because previous studies have found an unexpectedly strong link between these two populations (Zhu & Wu 2018; Bryan et al. 2019). Both transit and Doppler studies have shown that SEs exist around one-third of Sun-like stars, and that SEs are accompanied by CJs about one-third of the time — implying that one in nine Sun-like stars has both a SE and a CJ. This is interesting because 1/9 is similar to the overall occurrence rate of CJs found in Doppler surveys, unconditioned on the presence of SEs (Cumming et al. 2008; Mayor et al. 2011; Fernandes et al. 2019). The implication is that nearly all CJs are accompanied by SEs. Such a strong association must be a clue about the formation and evolution of these systems. It seems to contradict the scenario modeled by Izidoro et al. (2015) in which CJs block the migration of SEs, as well as the scenario of Ormel et al. (2017) in which CJs inhibit the formation of SEs by blocking the flux of pebbles from the outer regions of the protoplanetary disk. In either scenario, it would be rare to find both an inner SE and a CJ. On the other hand, a positive correlation would be expected if the close-in SEs form *in situ* from a massive disk (Chiang & Laughlin 2013; Schlaufman 2014).

Given the strong correlation between SEs and CJs, it is also of interest to understand their mutual inclinations. This serves as a probe of the degree of dynamical excitation, complementary to the orbital eccentricity. The mutual inclination is also important for understanding how the gravitational perturbations from the CJ have affected the properties of the inner SEs. Several theoretical works have shown that CJs on inclined orbits can dynamically heat the inner SE systems, increasing the inclination dispersion of the inner system or even destabilizing the orbits and reducing the multiplicity through collisions and ejections (Lai & Pu 2017; Huang et al. 2017; Gratia & Fabrycky 2017; Hansen 2017; Mustill et al. 2017; Becker & Adams 2017; Pu & Lai 2018). Indeed, some evidence has already been found that a subset of these compact systems are dy-

¹ We use the term “cold” as a simple way to distinguish these planets from the traditionally defined “hot Jupiters” ($a < 0.1$ AU) and “warm Jupiters” ($0.1 \text{ AU} < a < 1 \text{ AU}$). The terminology is not ideal because the actual planet Jupiter, at 5 AU, is colder than most of the known “cold Jupiters”. This may be why Dawson & Chiang (2014) preferred the name “balmy Jupiters”.

namically hot (Xie et al. 2016; Van Eylen et al. 2019; Zhu et al. 2018; Dai et al. 2018; Mills et al. 2019a). Knowledge of how, and how often, the inner systems are perturbed is essential for understanding the diversity of close-in SE systems.

This paper is organized as follows. Section 2 presents the simple and approximate calculation that inspired the more rigorous and thorough examination that is presented in the rest of the paper. Section 3 lays out the mathematical framework of the more complex calculation. Section 4 describes one of the key observational inputs: the occurrence rate of CJs around stars with inner SEs. Section 5 describes another crucial input: the construction of a sample of stars with transiting inner SEs, and a subsample that also has transiting CJs. Section 6 presents the results for the mutual inclination distribution and its dependence on the transit multiplicity of the inner system. Section 7 relates some tests we performed on the robustness of the results to reasonable variations in the analysis procedure. After our analysis was completed, we learned of an analysis with a similar goal by Herman et al. (2019). Section 8 presents a brief comparison between our work and theirs. Finally, Section 9 summarizes the results and relates them to other observations and theories for the architecture of compact systems of SEs.

2. SIMPLE CALCULATION

The *Kepler* database includes about 1,000 stars with at least one confirmed transiting inner super-Earth. As we will see in Section 4, the available Doppler data imply that about one-third of these SE systems should also harbor a cold Jupiter. If the SE and CJ orbital orientations were uncorrelated, then the transit probability for a CJ would be R_\star/a , where R_\star is the stellar radius and a is the orbital distance. If the period P is longer than the 4-year duration of the prime *Kepler* mission, the probability to transit during the mission is reduced by a factor of about $4 \text{ yr}/P$. This transit probability is about $1/500$ when averaged over the range of orbital periods of the observed CJs. Thus, if the orbits were uncorrelated, the expected number of stars with transiting SEs and transiting CJs would be about $1000/3/500$ or $2/3$. However, there are 3 known cases of transiting CJs in systems with inner SEs, as detailed in Section 5. This is 4.5 times larger than the expected value, indicating that the orbital orientations of SEs and CJs are correlated.

We can use this observation to place a rough constraint on the typical mutual inclination θ between the inner SEs and the outer CJ. Whenever an outer planet (with orbital distance a_{out}) and an inner planet (a_{in}) have a mutual inclination larger than R_\star/a_{in} , and the

inner planet is transiting, then the transit probability of the outer planet is larger than R_\star/a_{out} by a factor of approximately $1/\sin \theta$ (Ragozzine & Holman 2010). By setting this geometrical factor equal to the observed $4.5\times$ enhancement in the occurrence of transiting CJs in SE systems, we find

$$\frac{1}{\sin \theta} \approx 4.5 \longrightarrow \theta \approx 13^\circ. \quad (1)$$

Moreover, in all 3 cases in which transiting CJs have been found in this sample, there is more than one transiting inner SE. This is despite the fact that stars with multiple transiting SEs constitute only 1/3 of the sample. Thus, considering only the sample of multi-transiting SE systems, the observed occurrence of transiting CJs is larger than would be expected for uncorrelated orbits by a factor of 3×4.5 or 13.5. Using the equation above with 13.5 instead of 4.5, the typical mutual inclination is approximately 4° . As for the other 2/3 of the sample, consisting of single-transiting SE systems, the lack of any detections of transiting CJs is compatible with the assumption of uncorrelated orbits.

In short, these rough calculations indicate that the orbits of CJs have a typical inclination of $\sim 10^\circ$ with respect to inner SEs, and also that the inclination is smaller when the inner system is composed of multiple transiting SEs. The rest of this paper describes our effort to perform these calculations more rigorously and understand the limitations and implications of the results.

3. COMPLEX CALCULATION

We denote by \mathcal{S} the sample of *Kepler* stars with transiting inner SEs. The expected number of transiting CJs in this sample depends on both the probability that CJs exist in a system with SEs, as well as the probability distribution $p(\theta)$ for the angle between the orbits of the CJ and the SEs. We assume that $p(\theta)$ can be well modeled as a von Mises–Fisher distribution (Fisher 1953)

$$p(\theta|\kappa) d\theta \propto \exp(\kappa \cos \theta) \sin \theta d\theta, \quad 0 \leq \theta \leq \pi. \quad (2)$$

Here, $\kappa > 0$ is the concentration parameter, which is small for nearly isotropic distributions and large for distributions that are sharply peaked around $\theta = 0$. We prefer to parameterize the distribution in terms of $\sigma \equiv \kappa^{-1/2}$, because as $\sigma \rightarrow 0$ the distribution approaches the familiar Rayleigh distribution with scale parameter σ , for which the mode is σ , the mean is $(\pi/2)^{1/2}\sigma \approx 1.25\sigma$, and the root-mean-square value is $\sqrt{2}\sigma$. We will compute $p(n_{\text{tCJ}}|\sigma)$, the probability distribution for the number of transiting CJs in the sample, and compare it to $n_{\text{tCJ,obs}}(\mathcal{S})$, the observed number of

transiting CJs in the sample. In this way, we will determine the relative likelihood of different values of σ .

We calculate $p(n_{\text{tCJ}}|\sigma)$ via Monte Carlo simulation:

1. We assign one CJ to a fraction Z of randomly chosen stars in \mathcal{S} . This subset is denoted \mathcal{S}_{CJ} . The chosen fraction Z is based on the previous work of Zhu & Wu (2018) and Bryan et al. (2019), as described in Section 4. Each CJ is randomly assigned an orbital period $P_{\text{CJ},i}$ and eccentricity $e_{\text{CJ},i}$ based on the results of Doppler surveys, in a manner to be discussed in Section 4. The argument of periastron $\omega_{\text{CJ},i}$ is randomly drawn from a uniform distribution.
2. Each CJ in \mathcal{S}_{CJ} is also assigned an orbital inclination $I_{\text{CJ},i}$ relative to the line of sight. This is computed by drawing a mutual inclination θ_i from the probability distribution $p(\theta|\sigma)$, and combining it with the mean orbital inclination $I_{\text{SE},i}$ of the inner system of SEs:

$$\cos I_{\text{CJ},i} = \cos \theta_i \cos I_{\text{SE},i} + \sin \theta_i \sin I_{\text{SE},i} \cos \phi, \quad (3)$$

where ϕ is a phase angle randomly sampled from a uniform distribution. The relevant geometry is shown in Figure 1. The figure shows that the last term in the preceding equation should be $\cos(\phi_{\text{LOS}} - \phi_{\text{CJ}})$, which has the same distribution as the cosine of a uniformly distributed random variable under the assumptions that ϕ_{LOS} and ϕ_{CJ} are themselves uncorrelated and uniformly distributed.

We estimate I_{SE} using the reported values of orbital inclination that were determined by fitting the transit light curves. When there is more than one transiting inner planet, we set I_{SE} equal to the mean orbital inclination of all the planets.²

3. We check on whether or not each of the assigned CJs exhibits transits. We compute the impact parameter

$$b_{\text{CJ},i} = \frac{a_{\text{CJ},i}(P_{\text{CJ},i}, M_{\star,i}) \cos I_{\text{CJ},i}}{R_{\star,i}} \frac{1 - e_{\text{CJ},i}^2}{1 + e_{\text{CJ},i} \sin \omega_{\text{CJ},i}},$$

² Strictly speaking, there is ambiguity in this procedure because of the degeneracy between I and $180^\circ - I$ when fitting transit light curves. We always choose values of I to be less than 90° , motivated by the finding of Fabrycky et al. (2014) that wider-orbiting planets tend to have higher transit impact parameters, indicating that multiple transiting SEs tend to have mutual inclinations of at most a few degrees. In any case, this choice only affects $p(n_{\text{tCJ}}|\sigma)$ for $\sigma \lesssim$ a few degrees, and our conclusions will not be sensitive to the difference in this region.

and set $n_{\text{tCJ},i} = 0$ if $b_{\text{CJ},i} > 1$. If $b_{\text{CJ},i} < 1$, we also compute the total duration $T_{\text{obs},i}$ of observations of the host star, by multiplying the timespan of the *Kepler* data by the duty cycle. When $T_{\text{obs},i} > P_{\text{CJ},i}$, we set $n_{\text{tCJ},i} = 1$. When $T_{\text{obs},i} < P_{\text{CJ},i}$, the transit of the CJ might fall outside the observing duration; we set $n_{\text{tCJ},i} = 1$ with probability $T_{\text{obs},i}/P_{\text{CJ},i}$ and $n_{\text{tCJ},i} = 0$ otherwise. Finally, we compute

$$n_{\text{tCJ}}|\sigma = \sum_{i \in \mathcal{S}_{\text{CJ}}} n_{\text{tCJ},i}. \quad (4)$$

Here we have assumed that the transits of the simulated CJs are always detected whenever they occur. As explained in Section 5, we will choose the sample \mathcal{S} so that this assumption is justified.

For each value of σ , we repeat these steps for different values of Z that are compatible with the observational uncertainty. The Monte Carlo simulation is repeated for a range of possible values of σ , thereby delivering the desired probability distribution $p(n_{\text{tCJ}}|\sigma)$. Finally, we compute the likelihood function $\mathcal{L}(\sigma) \equiv p(n_{\text{tCJ,obs}}|\sigma)$ in order to draw inferences about the mutual inclination distribution.

4. OCCURRENCE RATE OF COLD JUPITERS IN SUPER-EARTH SYSTEMS

Zhu & Wu (2018) and Bryan et al. (2019) independently analyzed the occurrence rate of Doppler CJs around stars with inner SEs, based on samples of SE systems drawn from both the *Kepler* transit survey and from precise Doppler surveys. Their key results are summarized in Table 1. There are a number of differences between the two analyses, including the types of host stars considered, the adopted definitions of SEs and CJs, and the treatment of candidate CJs for which the available Doppler data do not span a full orbit. Nevertheless, the occurrence rates derived by these authors are consistent with each other. The rates derived from the sample of Doppler SEs and from the sample of transiting SEs do not show significant differences, either. For our purpose, we adopted $Z = (34 \pm 7)\%$, based on the results of Bryan et al. (2019) for the narrowest ranges of mass and semi-major axis they considered (i.e., the smallest amount of extrapolation).

In constructing our sample \mathcal{S} , we needed to match the definitions of CJs and SEs as closely as possible to the definitions that were adopted by Bryan et al. (2019). For this reason, we defined inner SEs as planets with radii $r = 1\text{--}4 R_{\oplus}$ and orbital periods $P < 130$ days

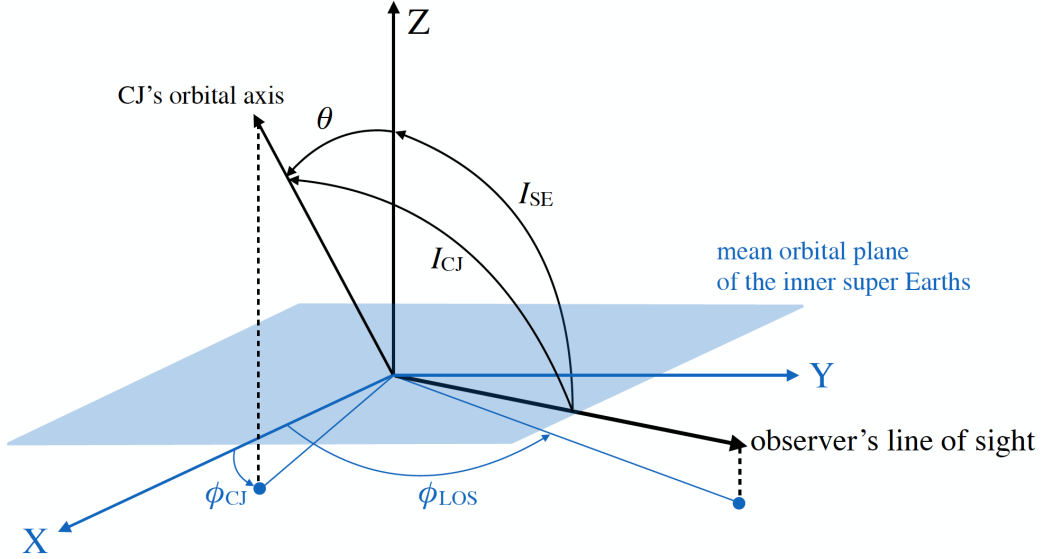


Figure 1. Geometry of the system. The angle θ is the mutual inclination between the orbit of the cold Jupiter and the mean orbital plane of the inner super-Earths. We are ignorant about the phase angles ϕ_{CJ} and ϕ_{LOS} .

Table 1. Estimated occurrence rate of cold Jupiters (CJs) around stars with inner super-Earths (SEs), drawn from the literature.

	Definition of SEs	Definition of CJs	Fraction Z
<i>Zhu & Wu (2018), FGK stars</i>			
Doppler	$m \sin i < 20 M_{\oplus}, P < 400$ days	$m \sin i > 95 M_{\oplus} (0.3 M_{Jup}), P \gtrsim 1$ yr	$10/32 = (32 \pm 8)\%$
transit	$r = 1-4 R_{\oplus}, P < 400$ days	$m \sin i > 95 M_{\oplus} (0.3 M_{Jup}), P \gtrsim 1$ yr	$7/22 = (33 \pm 10)\%$
combined	$r = 1-4 R_{\oplus}$ or $m \sin i < 20 M_{\oplus}, P < 400$ days	$m \sin i > 95 M_{\oplus} (0.3 M_{Jup}), P \gtrsim 1$ yr	$17/54 = (32 \pm 6)\%$
<i>Bryan et al. (2019), FGKM stars</i>			
Doppler	$m \sin i = 1-10 M_{\oplus}, a < 0.5$ AU	$m = 0.5-20 M_{Jup}, a = 1-20$ AU ($P \simeq 1-90$ yr)	$34^{+11}_{-10}\%$
transit	$r = 1-4 R_{\oplus}, a < 0.5$ AU	$m = 0.5-20 M_{Jup}, a = 1-20$ AU ($P \simeq 1-90$ yr)	$41^{+10}_{-10}\%$
combined	$r = 1-4 R_{\oplus}$ or $m \sin i = 1-10 M_{\oplus}, a < 0.5$ AU	$m = 0.5-20 M_{Jup}, a = 1-20$ AU ($P \simeq 1-90$ yr)	$(39 \pm 7)\%$
combined 2	$r = 1-4 R_{\oplus}$ or $m \sin i = 1-10 M_{\oplus}, a < 0.5$ AU	$m = 0.5-20 M_{Jup}, a = 1-10$ AU ($P \simeq 1-30$ yr)	$(38 \pm 7)\%$
combined 3	$r = 1-4 R_{\oplus}$ or $m \sin i = 1-10 M_{\oplus}, a < 0.5$ AU	$m = 1-13 M_{Jup}, a = 1-10$ AU ($P \simeq 1-30$ yr)	$(34 \pm 7)\%$

($a < 0.5$ AU for a solar-mass star).³ A complication that arose when defining CJs is that Bryan et al. (2019) used a mass-based definition while we needed to use a radius-based definition. Fortunately, the mass-radius relation for giant planets is well understood: the radius hardly changes at all with mass, for objects between 0.3 and $30 M_{Jup}$. The smallest known planet in this mass range with both well-determined mass and radius has a radius of $7.7 \pm 0.4 R_{\oplus}$ (K2-60 b, Eigmüller et al. 2017).

³ Although Zhu & Wu (2018) included SEs with periods as long as 400 days, the difference is minor because there are very few *Kepler* transiting SEs with periods between 130 and 400 days.

Therefore, we defined CJs as planets with $r > 7.5 R_{\oplus}$ and $P = 1$ to 30 yr. An unavoidable problem with this definition is that it includes brown dwarfs with masses $> 13 M_{Jup}$, which were not always counted as planets in the Doppler surveys, but this is a minor problem because brown dwarfs are much less common than giant planets in this period range (e.g., Grether & Lineweaver 2006). Our definition also inadvertently includes any low-mass, low-density planets that are less massive than about $0.3 M_{Jup}$ and larger than $7.5 R_{\oplus}$. Such objects are known to exist in < 1 yr orbits, but they are less common than ordinary SEs by at least an order of magnitude (Petigura et al. 2018). For our analysis we had to assume that their occurrence rate is also much lower for

orbital periods longer than 1 yr, than that of traditional giant planets (i.e., 1/3 around SEs). If this assumption is mistaken, then our analysis will underestimate the typical mutual inclination.

Next, we needed to assign orbital periods and eccentricities to the simulated CJs. Since previous studies have concluded that almost all CJs are associated with inner SEs, the properties of CJs around SEs should be similar to the properties of CJs in general that have been derived from Doppler surveys. [Zhu & Wu \(2018\)](#) verified that this is the case. To model the period distribution, we relied on the results of [Fernandes et al. \(2019\)](#), based on long-term surveys with the High Accuracy Radial-velocity Planet Searcher (HARPS, [Mayor et al. 2011](#)). The simplest model for the period distribution that they found to be consistent with the population of giant planets with $P \gtrsim 100$ days is

$$p(\ln P) d \ln P \propto \mathcal{N}(\ln P_0, \sigma_{\ln P}) d \ln P, \quad (5)$$

where $\mathcal{N}(\mu, \sigma)$ denotes a normal distribution with mean μ and dispersion σ , and the two constants are $P_0 = (919 \pm 105)$ days and $\sigma_{\ln P} = 1.46$ (see their Figure 3). For the probability distribution of orbital eccentricity, we followed [Kipping \(2013\)](#) by adopting a beta distribution,

$$p(e) de \propto e^{a-1}(1-e)^{b-1}, \quad (6)$$

with $a = 1.12$ and $b = 3.09$.

Our model does not allow a star to have more than one wide-orbiting giant planet. The possible multiplicity of CJs is often ignored in studies of planet occurrence from Doppler surveys, and was handled differently by [Zhu & Wu \(2018\)](#) and [Bryan et al. \(2019\)](#). The former group counted the number of stars with at least one CJ, while the latter group included only the innermost CJs and verified that their results were not sensitive to which of the inner or outer planets were included. By ignoring the possibility of a second CJ, our analysis underestimates the probability that a star will have a transiting CJ, but we expect this to be a minor error because any more distant CJs will have lower transit probabilities — and as we will see later, no star in our sample has more than one transiting CJ. This possible source of systematic error will be addressed further in Section 7.5.

5. THE SAMPLE OF STARS WITH TRANSITING SUPER EARTHS

Here we define the sample \mathcal{S} of stars hosting close-in SEs. As discussed in the previous section, the sample needs to satisfy the following criteria:

1. The stars have reliably detected SEs similar to the ones studied by [Zhu & Wu \(2018\)](#) and [Bryan et al. \(2019\)](#).

2. The detection of a transiting CJ would be straightforward, consistent with the assumption that all transiting CJs around the stars would have been detected.
3. The stars are similar in their basic properties to the ones studied by [Zhu & Wu \(2018\)](#) and [Bryan et al. \(2019\)](#).

We began with the list of 177,911 *Kepler* stars presented by [Berger et al. \(2018\)](#), for which stellar radii were well constrained based on the parallax from the *Gaia* Data Release 2 ([Gaia Collaboration et al. 2018](#)) and the effective temperature determined from various sources. For some of the stars, we adopted the improved (spectroscopic) determinations of effective temperature from the work of [Kawahara & Masuda \(2019\)](#), and updated the determination of the stellar radius. These stars were cross-matched with the *Kepler* Object of Interest (KOI) catalog, Data Release 25 ([Thompson et al. 2018](#)), and the planetary radii r were assigned based on the radius ratio in the catalog and the updated stellar radii.

We defined the sample \mathcal{S} of *Kepler* stars with inner SEs based on the following criteria:

1. The star is not associated with any “false positive” planets reported in the KOI catalog.
2. The star has at least one confirmed inner SE, i.e., one planet with $P < 130$ days and $1 < r/R_{\oplus} < 4$. We also imposed a restriction on the transit impact parameter, $b < 0.9$, to eliminate cases in which the planet radius cannot be measured reliably.
3. The star has no detected transiting planets with $P < 130$ days and $r > 4 R_{\oplus}$. This is because of the evidence that stars with hot or warm giant planets may have higher occurrence rates of CJs ([Bryan et al. 2016](#)). This criterion removes only a small number of stars because hot/warm giant planets are intrinsically rare.
4. The transit depth expected for a $6 R_{\oplus}$ planet is at least 10 times larger than the Combined Differential Photometric Precision (CDPP, [Koch et al. 2010](#)) computed for the 15 hr timescale. This is to ensure that transiting CJs would have been easily detected, although this condition was almost always satisfied because the star was already required to have a detected transiting SE. Only 21 stars were dropped at this stage.

The resulting sample consists of 1,046 stars hosting a total of 1,421 SEs. Among them, 651 stars have a single transiting SE, and 395 stars have multiple transiting

planets including SEs as defined above. Our main analysis is based only on this sample of stars with confirmed transiting SEs, although in Section 7.1 we discuss how the results would change if we include stars hosting candidate transiting SEs.

Figures 2 and 3 compare the stellar properties of our sample with those of the stars analyzed by Zhu & Wu (2018) and Bryan et al. (2019) (collected from the NASA exoplanet archive⁴). The figures show that Zhu & Wu (2018) focused on FGK stars, while $\approx 20\%$ of the sample of Bryan et al. (2019) were M dwarfs. In addition, the stars from the sample of Bryan et al. (2019) have a lower mean iron abundance than those in the sample of Zhu & Wu (2018), by 0.06 dex. Nevertheless, the two groups derived occurrence rates for CJs outside close-in SEs that are consistent with each other, as summarized in Table 1. The properties of our sample overlap with those of the two previous samples. We also see no significant difference between the properties of stars with single transiting planets and those with multiple transiting planets.

5.1. How Many of Them Have Transiting CJs?

We consulted the catalog of Kawahara & Masuda (2019) to identify the stars in our sample \mathcal{S} that have transiting CJs that meet the criteria $r > 7.5 R_{\oplus}$ and $1 \text{ yr} < P < 30 \text{ yr}$. The catalog includes all of the long-period transiting planet candidates known from the prime *Kepler* mission. We found $n_{\text{tCJ,obs}} = 3$ for the confirmed SE sample: the CJs around KIC 3218908 and 11709124 were originally reported by Uehara et al. (2016) and the CJ around KIC 3239945 was validated by Kipping et al. (2016). These are listed in Table 2 in boldface type. Although two of them show only one transit in the *Kepler* data, their transit durations combined with stellar radii indicate that their periods are in the range of interest. They all have three or more inner transiting planets, and they were all detected both by visual inspection (Uehara et al. 2016) and through an automated search (Foreman-Mackey et al. 2016).

We note that KIC 3218908 was classified as a photometric binary by Berger et al. (2018) because the calculated stellar radius of $1.22 R_{\odot}$ was larger than expected for the estimated effective temperature of 4938 K. However, a more recent spectroscopic determination of the effective temperature is 5578 K (Kawahara & Masuda 2019), placing the star closer to the main sequence (see Figure 2) and making this star less anomalous. In any case, the system would still meet our criteria for the

“CJ+SE” sample even if the transit signal was diluted by an unresolved companion with a similar luminosity.

The super-Earth sample \mathcal{S} contains about 1,000 stars and its composition would not change substantially if we made small changes to the selection criteria. However, since the number of transiting CJs in this sample is only 3, we need to be more careful about the effects on the results of any minor changes in the selection criteria. To check on this, Table 2 has a complete listing of all the stars known to have both long-period transiting planets and inner transiting planets. Some of the entries are not counted in $n_{\text{tCJ,obs}}$ because the outer planets are too small. Those dropped all have $r \lesssim 6.4 R_{\oplus}$ (KIC 10187159); empirically, such planets are very likely to be less massive than $0.3 M_{\text{Jup}}$, and thereby do not fall inside the definitions of CJs for which the conditional occurrence is known. The italicized entries are not counted in $n_{\text{tCJ,obs}}$ because the star is not included in the SE sample \mathcal{S} . The transiting CJs around KIC 9663113 and KIC 6191521 were not included in \mathcal{S} because the inner transiting planets are giant planets. Thus, $n_{\text{tCJ,obs}}$ in the confirmed SE sample appears to be robust against small changes in the definitions of close-in SEs and CJs.

We also checked for any stellar companions found by the Robo-AO *Kepler* survey (Ziegler et al. 2018). Companions within 4 arcsec were detected for KIC 9663113 (KOI-179) and KIC 8636333 (KOI-3349), but the associated corrections to the planet radii are either negligibly small (if the planet orbits the primary star), or so large that the system becomes physically implausible or irrelevant to our purpose (if the planet orbits the secondary star). The other stars in Table 2 have no detected companions.

We emphasize that this list needs to be complete only for Jupiter-sized transiting planets in our sample of KOI stars with close-in SEs, on which our analysis is solely conditioned. This is a much less stringent requirement than performing a complete search of long-period transiting planets around generic *Kepler* stars. Our search need not be complete for planets smaller than about $7 R_{\oplus}$, nor for planets around stars without transiting SEs (i.e., the vast majority of the *Kepler* stars). The light curves of KOI stars have been thoroughly examined via both visual inspection (Uehara et al. 2016) and automated algorithms (Foreman-Mackey et al. 2016; Herman et al. 2019), and the resulting samples of transiting Jupiter-sized planets around confirmed KOIs agree with each other. It has also been shown that the gaps in the light curves that occur when the signals of inner transiting planets are removed have only a minor effect on the detectability of long-period transiting planets (Schmitt et al. 2017). Thus we believe we have counted all the rel-

⁴ <https://exoplanetarchive.ipac.caltech.edu>. A few stars for which no information was available were ignored.

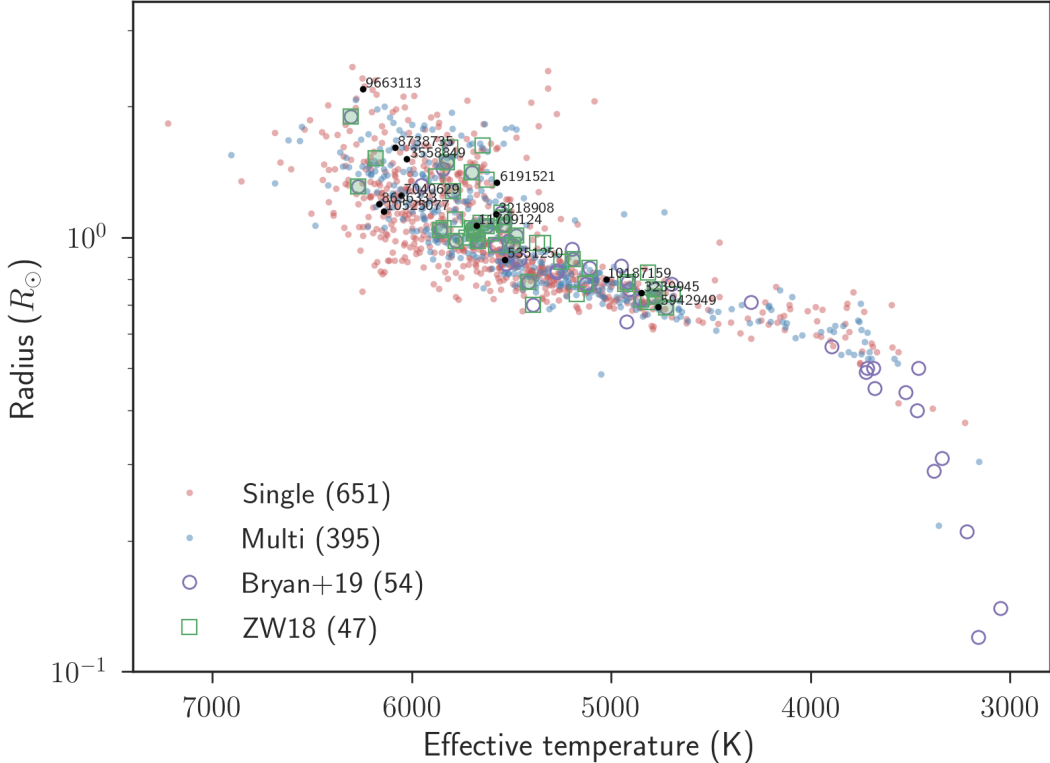


Figure 2. The radius and effective temperature of the stars hosting SEs from our sample and two previously studied samples. Red and blue dots represent stars from our sample with a single transiting planet and with multiple transiting planets, respectively. Purple open circles and green open squares are super-Earth hosts analyzed by Bryan et al. (2019) and Zhu & Wu (2018), respectively. Black dots represent all the *Kepler* stars for which transits of both a long-period giant planet and an inner super-Earth have been detected (Table 2).

evant transiting Jupiter-sized planets around the stars in our SE sample. Nevertheless, we discuss possible effects of detection incompleteness in Section 7.2.

6. RESULTS

Using the CJ occurrence from Section 4 and the transit sample defined in Section 5, we computed $\mathcal{L}(\sigma)$ for 15 values of σ spanning the range from 1 deg to 100 deg, spaced equally in the logarithm of σ . For $\sigma \lesssim 10$ deg, the model inclination distribution is essentially a Rayleigh distribution, while for $\sigma = 100$ deg, the distribution is nearly isotropic. We interpolated the values of $\mathcal{L}(\sigma)$ using a spline function, then determined the maximum-likelihood value of σ as well as the intervals corresponding to $\Delta \ln \mathcal{L}(\sigma) = -1/2$ and -2 . Table 3 gives the results. The top panels of Figure 4 show the functions $p(n_{\text{tCJ}}|\sigma)$ for various choices of σ (left), along with the log-likelihood function $\ln \mathcal{L}(\sigma) \equiv p(n_{\text{tCJ}} = n_{\text{tCJ,obs}}|\sigma)$ (right).

The maximum-likelihood value of σ is close to 10 deg, consistent with the approximate derivation given in Section 2. The 95%-confidence lower limit is 3.5° , which is somewhat larger than the typical mutual inclinations

that have been inferred for compact multi-transiting systems ($\sigma \sim$ a few degrees; Fabrycky et al. 2014; Fang & Margot 2012). Had σ been equal to 2° , for example, we would have most likely detected 10 transiting CJs (see the green curve in the top left panel of Figure 4).

The middle and lower panels of Figure 4 show the results for the subset of \mathcal{S} with multiple transiting inner planets including SEs (“multis”), and the subset with one transiting SE (“singles”). Inspection of these results shows that the relatively large σ inferred for the whole sample is mainly driven by the subset of singles, while the multis favor lower values of σ . When only the singles are analyzed, the null detection of any transiting CJs implies $\sigma > 8$ deg with 95% confidence. This reflects the fact that the upper limit on the CJ transit probability inferred from the null detection is comparable to the value expected for random orbital orientations (Section 2). This value of σ is larger than the mutual inclinations that have been inferred for shorter-period multi-transiting systems, as well as those of the Solar System planets. In fact, the same is also true for the subset of \mathcal{S} having only one *or two* transiting planets, because no

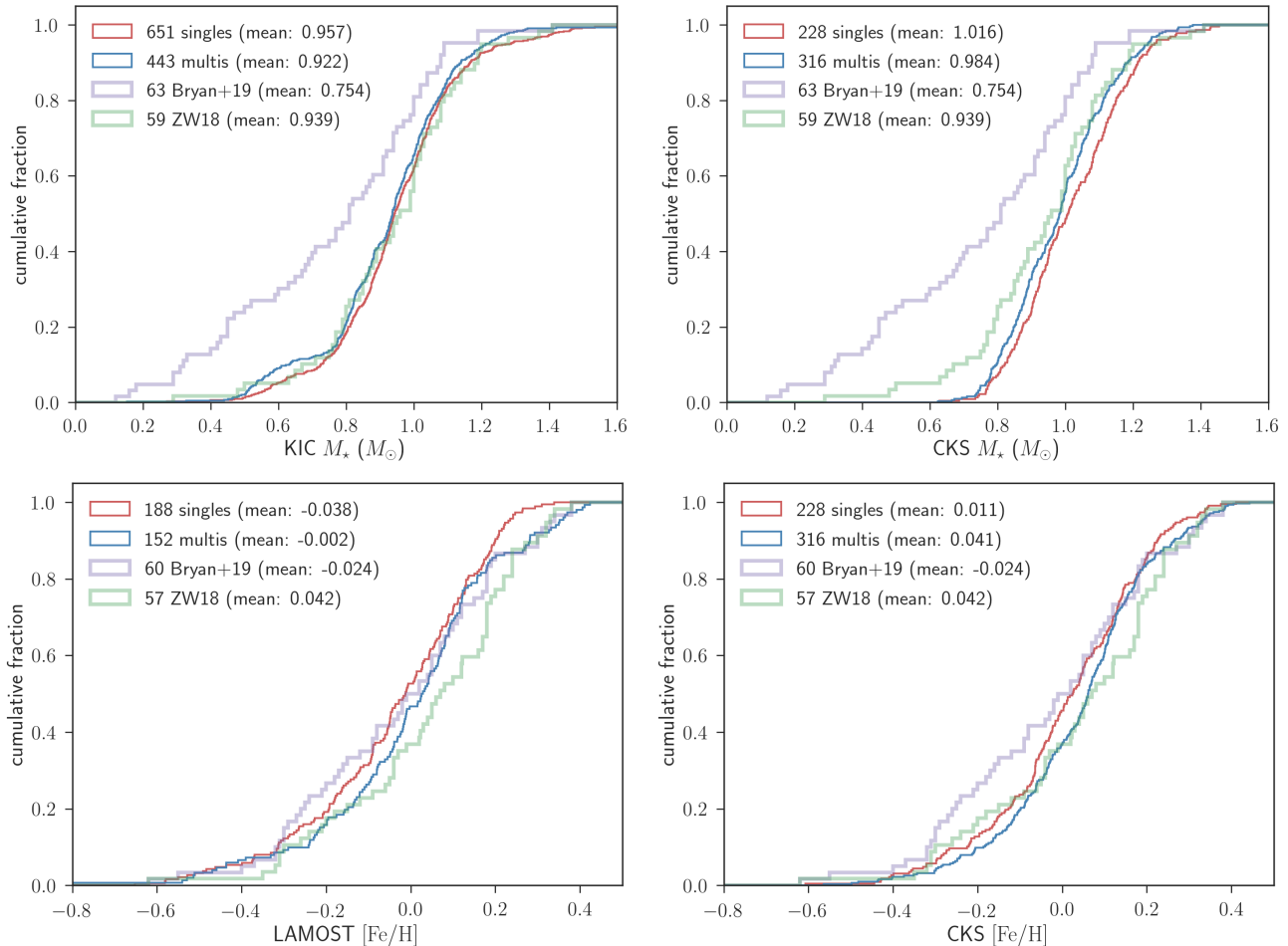


Figure 3. Distributions of stellar mass and $[Fe/H]$ for the stars in our sample and the previously analyzed samples of [Zhu & Wu \(2018\)](#) and [Bryan et al. \(2019\)](#). The data for the previously analyzed samples were taken from the NASA exoplanet archive. Those for our sample stars are from difference sources: *Top left* — stellar masses from the *Kepler* Input Catalog. *Top right* — stellar masses from the California *Kepler* survey (CKS; [Petigura et al. 2017](#); [Johnson et al. 2017](#)). *Bottom left* — $[Fe/H]$ from LAMOST ([Cui et al. 2012](#); [Luo et al. 2015](#)) DR 4. *Bottom-right* — $[Fe/H]$ from the CKS.

transiting CJs were found in that subset, either. The result in this case is $\sigma > 11$ deg.

On the other hand, when analyzing only the multis, the most likely value of σ is 3.9° , again consistent with the derivation in Section 2. This result follows from the detection of three transiting CJs around stars with multiple transiting SEs, which is an order of magnitude more than one would expect if the mutual inclinations were random. Since all three of the detections were around stars with three or more transiting SEs, the results suggest that the mutual inclinations between CJs and high-transit-multiplicity (i.e., 3 or more) systems of SEs are less than a few degrees, comparable to the mutual inclinations in the SE system and the Solar System.

7. TESTS FOR ROBUSTNESS

7.1. What About Candidate Transiting SEs?

How do the results change if we include candidate transiting SEs, rather than accepting only confirmed transiting SEs? If we admit candidate SEs to the sample, the total number of stars in \mathcal{S} grows to 1,721, and the total number of transiting SEs becomes 2,335. Of the stars, 1,257 have only one detected transiting SE, and 464 stars have multiple transiting planets including SEs.

This enlarged sample includes one clear case of a transiting cold Jupiter around KIC 5942949 ([Uehara et al. 2016](#), Table 2). There is also one borderline case: KIC 3558849. The star has a transiting cold Jupiter, but the inner planet candidate in this system (KOI-4307.01) does not quite fit the definition of an inner super-Earth: its period of 161 days is longer than the

Table 2. Long-period Transiting Planets with Inner Transiting Planets.

KIC	KOI	<i>Kepler</i>	radius (R_{\oplus})	orbital period (days)	eccentricity	inner KOIs
<i>(confirmed KOIs)</i>						
11709124	435	154	$10.26^{+0.34}_{-0.36}$	1250^{+490}_{-240}	$0.15^{+0.22}_{-0.11}$	435.04 (1.6 R_{\oplus} , 3.93 days) 435.06 (1.4 R_{\oplus} , 9.92 days) 435.01 (4.4 R_{\oplus} , 20.5 days) 435.03 (2.6 R_{\oplus} , 33.0 days) 435.05 (3.3 R_{\oplus} , 62.3 days)
3239945	490	167	$9.99^{+0.14}_{-0.15}$	$1071.2321^{+0.0010}_{-0.0009}$	$0.06^{+0.13}_{-0.04}$	490.01 (1.5 R_{\oplus} , 4.39 days) 490.03 (1.5 R_{\oplus} , 7.41 days) 490.04 (1.2 R_{\oplus} , 21.8 days)
<i>9663113</i>	179	458	9.62 ± 0.39	572.382 ± 0.006	$0.15^{+0.16}_{-0.10}$	179.01 (7.2 R_{\oplus} , 20.7 days)
<i>6191521</i>	847	700	$9.55^{+0.51}_{-0.48}$	1106.238 ± 0.006	$0.10^{+0.15}_{-0.07}$	847.01 (8.2 R_{\oplus} , 80.9 days)
3218908	1108	770	$8.03^{+0.34}_{-0.31}$	1290^{+870}_{-340}	$0.15^{+0.19}_{-0.10}$	1108.01 (3.2 R_{\oplus} , 18.9 days) 1108.02 (1.4 R_{\oplus} , 1.48 days) 1108.03 (1.8 R_{\oplus} , 4.15 days)
10187159	1870	989	$6.39^{+0.19}_{-0.17}$	1310^{+640}_{-240}	$0.40^{+0.11}_{-0.10}$	1870.01 (2.1 R_{\oplus} , 8.0 days)
8738735	693	214	$5.83^{+0.37}_{-0.27}$	1390^{+1190}_{-370}	$0.17^{+0.18}_{-0.11}$	693.02 (3.2 R_{\oplus} , 15.7 days) 693.01 (3.0 R_{\oplus} , 28.8 days)
8636333	3349	1475	$5.74^{+0.43}_{-0.39}$	2030^{+1490}_{-560}	$0.29^{+0.23}_{-0.20}$	3349.01 (2.8 R_{\oplus} , 82.2 days)
7040629	671	208	3.30 ± 0.16	5690^{+4000}_{-2970}	$0.22^{+0.22}_{-0.15}$	671.01 (1.5 R_{\oplus} , 4.23 days) 671.02 (1.4 R_{\oplus} , 7.47 days) 671.04 (1.2 R_{\oplus} , 11.1 days) 671.03 (1.4 R_{\oplus} , 16.3 days)
<i>5351250</i>	408	150	$3.3^{+0.19}_{-0.17}$	637.21 ± 0.02	$0.14^{+0.23}_{-0.10}$	408.04 (1.2 R_{\oplus} , 3.43 days) 408.01 (3.3 R_{\oplus} , 7.38 days) 408.02 (2.7 R_{\oplus} , 12.6 days) 408.03 (3.1 R_{\oplus} , 30.8 days) 408.05 (2.0 R_{\oplus} , 93.8 days, FP)
<i>(candidate KOIs)</i>						
5942949	2525	...	$11.64^{+2.14}_{-0.65}$	1550^{+1010}_{-280}	$0.26^{+0.21}_{-0.13}$	2525.01 (1.9 R_{\oplus} , 57.3 days)
<i>3558849</i>	4307	...	$10.19^{+0.40}_{-0.35}$	1650^{+710}_{-260}	$0.54^{+0.09}_{-0.08}$	4307.01 (3.4 R_{\oplus} , 161 days)
10525077	5800	459 [†]	$5.80^{+0.29}_{-0.25}$	$427.040^{+0.005}_{-0.004}$	$0.46^{+0.14}_{-0.09}$	5800.01 (1.5 R_{\oplus} , 11.0 days)

NOTE—The radius, orbital period, and eccentricity of the long-period planets from the analysis of transit light curves of Kawahara & Masuda (2019). The radii of the inner KOIs have been updated from the catalog values following the procedure in Section 5.

[†]The star has a *Kepler* number because the long-period transiting planet listed here has been validated by Wang et al. (2015); its period could be twice as long as the value here because of the data gap in the middle of the two detected transits. The inner candidate KOI-5800.01 has not been confirmed, and so we included this star in the candidate SE sample.

cutoff value of 130 days.⁵ However, the period is not

too much larger than the cutoff value, and it is within the range of < 400 days adopted by Zhu et al. (2018).

⁵ The SE candidate was reported by Morton et al. (2016) to have a 67% false-positive probability because the transit light curve is V-shaped instead of having a flat bottom. However, this may partly be due to possible long-term TTVs as reported by Kane et al. (2019). The existence of TTVs not only increases the prob-

ability that the planet is genuine, but also helps to explain why the transit profile was thought to be V-shaped: unmodeled TTVs tend to make the phase-folded light curve appear to have longer ingress and egress durations.

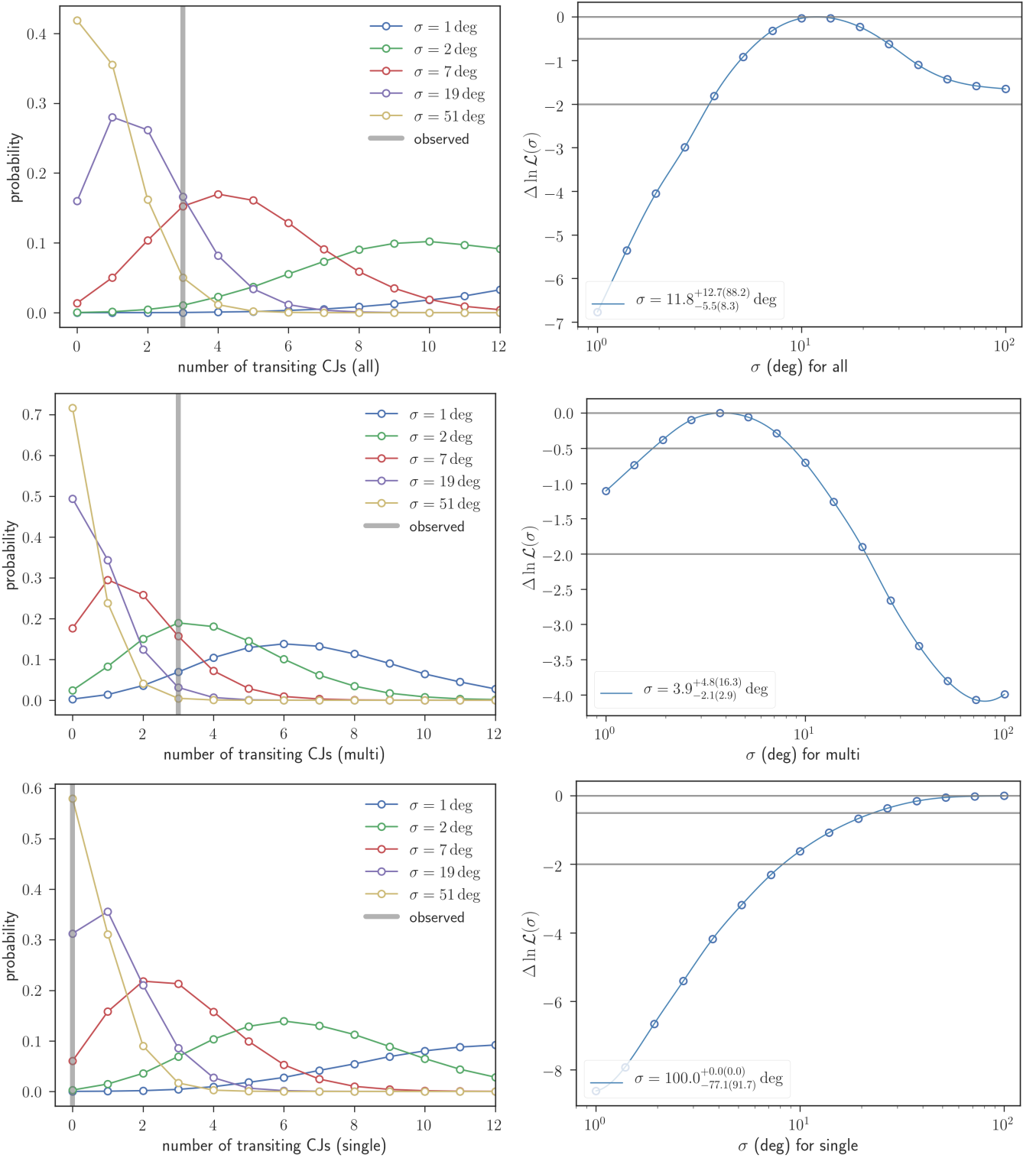


Figure 4. *Left* — $p(n_{\text{tCJ}}|\sigma)$ for the whole confirmed SE sample (top), subset with transit multis (middle), and that with transit singles (bottom). *Right* — The log-likelihood $\ln \mathcal{L}(\sigma)$ relative to the maximum value. Circles are values from simulations, and the solid lines interpolate them.

Table 3. Values of σ (degrees) for the confirmed SE sample.

	confirmed SE	
	Max. Likelihood	95% conf. limit
all stars ($n_{\text{in}} \geq 1$)	$11.8^{+12.7}_{-5.5}$	> 3.5
transit multis ($n_{\text{in}} > 1$)	$3.9^{+4.8}_{-2.1}$	< 20
transit singles ($n_{\text{in}} = 1$)	> 23	> 8.3
$n_{\text{in}} \geq 3$	< 2.5	< 6.6
$n_{\text{in}} = 1$ or 2	> 27	> 11

NOTE— n_{in} is the number of all transiting planets (confirmed and candidate KOIs) with periods shorter than 130 days. Lower limits are reported when the interval includes $\sigma = 100$ deg. Upper limits are reported when the interval includes 1 deg.

Because the period cutoff is rather arbitrary, we decided to analyze both of the cases $n_{\text{tCJ,obs}} = 4$ and 5 with and without KIC 3558849, and confirmed that the results are not sensitive to this difference.

Table 4 gives the results. The lower limits on σ for transit singles (and doubles) are slightly weaker, but are similar to the results obtained from the confirmed-only sample. This is because the increase in the number of detected transiting CJs around transit singles (one or two) is consistent with the increase in the sample size. The number of stars with transit multis remained mostly unchanged, and so σ increased only slightly.

7.2. What If Some Transiting CJs Were Missed?

We believe that our sample of transiting CJs is complete: the results of both automated searches and visual inspection were in agreement for this population, and their signals are 10 or more times larger than those from the inner planets that were also detected around these stars. Nevertheless, we decided to check on how serious the systematic error might be if the sample were incomplete.

We repeated our analysis of the confirmed sample, after artificially reducing the detectability of transiting CJs to be 60% in step 3 of Section 3. This choice was based on the completeness estimate for Jupiter-sized planets using the automated pipeline (Foreman-Mackey et al. 2016; Herman et al. 2019), and is conservative considering that the orbital periods of actual transiting CJs will be at the shorter end of the range they considered (≈ 2 – 20 yr). Table 5 shows the results: the values of σ are generally smaller, because a larger number of transiting CJs is allowed. Nevertheless, the basic conclusions are the same. This is because our constraint on σ relies on the observed 5 – $15\times$ boost in the transit probability

of cold Jupiters above the probability expected for uncorrelated orbits. This makes the results insensitive to $\mathcal{O}(10\%)$ changes in the number of detections.

7.3. Are CJs More Common Around Transit Multis?

We have assumed that the intrinsic occurrence rate of CJs is the same for all stars with transiting SEs, regardless of whether there is only a single transiting SE or multiple transiting SEs. We found the occurrence of transiting CJs around stars with a single transiting SE to be lower by a factor of $\gtrsim 5$ than the occurrence around stars with multiple transiting SEs. The results indicate that the mutual inclination between the CJ and the SEs is lower when there are multiple transiting SEs. However, if the intrinsic occurrence rate of CJs around stars with only a single transiting SE is $5\times$ lower than the rate of CJs around stars with multiple transiting SEs, then we would see fewer transiting CJs around transit singles even if the mutual inclination distribution were the same for all systems.

The SE samples of Zhu & Wu (2018) and Bryan et al. (2019) include stars with both single- and multi-transiting SEs. Although the subsamples are small, a difference in occurrence by a factor of 5 is disfavored by the data. In the transit sample of Zhu & Wu (2018), $7/22 = 32\%$ of the SE systems have CJs. The fraction for inner transit singles is $5/10 = (50 \pm 14)\%$, and that for inner transit multis is $2/12 = 20^{+12}_{-9}\%$. At face value, then, the transit singles could have a *higher* occurrence of CJs, and our results would require an even larger difference in the mutual inclinations between transit singles and multis — although the difference is less than the two-sigma level. In the Doppler sample of Zhu & Wu (2018), for which the intrinsic multiplicity (rather than transit multiplicity) is known, the CJ fraction around single SEs is $9/28 = (33 \pm 7)\%$, and that around multis is $3/11 = (30^{+13}_{-12})\%$. There is no evidence for any difference.

We also note that transit singles and multis generally have similar properties in terms of orbital periods, planetary radii, and stellar properties (Weiss et al. 2018). In addition, similar fractions of them show TTVs, suggesting that there is not a very large difference in their intrinsic multiplicities including non-transiting planets (Zhu et al. 2018). These observations support the assumption that the transit singles and multis share the same basic architecture except for mutual inclinations. The preceding comparison of the conditional CJ occurrences further supports this notion.

Finally, we checked for any differences in the metallicity distribution between the stars with a single transiting SE and those with multiple transiting SEs. This is

Table 4. Values of σ (degrees) for the confirmed + candidate SE sample.

	including KIC 3558849		not including KIC 3558849	
	Max. Likelihood	95% conf. limit	Max. Likelihood	95% conf. limit
all stars ($n_{\text{in}} \geq 1$)	$12.1^{+9.0}_{-4.6}$	[4.5, 42.6]	$15.7^{+13.0}_{-6.6}$	> 5.4
transit multis ($n_{\text{in}} > 1$)	$4.8^{+5.6}_{-2.6}$	< 24	$4.8^{+5.6}_{-2.6}$	< 24
transit singles ($n_{\text{in}} = 1$)	> 12	> 6.2	> 19	> 9.1
$n_{\text{in}} \geq 3$	< 2.6	< 6.9	< 2.6	< 6.9
$n_{\text{in}} = 1$ or 2	> 15	> 7.9	> 24	> 11

NOTE— n_{in} is the number of all transiting planets (confirmed and candidate KOIs) inside 130 days. Lower limits are reported when the interval includes $\sigma = 100$ deg. Upper limits are reported when the interval includes 1 deg.**Table 5.** Values of σ (degrees) Inferred for the Confirmed SE Sample, assuming that the detection completeness for transiting CJs is 60%.

	confirmed SE	
	Max. Likelihood	95% conf. limit
all stars ($n_{\text{in}} \geq 1$)	$6.9^{+7.4}_{-3.4}$	[1.4, 33.4]
transit multis ($n_{\text{in}} > 1$)	< 4.9	< 11.8
transit singles ($n_{\text{in}} = 1$)	> 17	> 5
$n_{\text{in}} \geq 3$	< 2.0	< 4.9
$n_{\text{in}} = 1$ or 2	> 21	> 7

NOTE— n_{in} is the number of all transiting planets (confirmed and candidate KOIs) inside 130 days. Lower limits are reported when the interval includes $\sigma = 100$ deg. Upper limits are reported when the interval includes 1 deg.

because high metallicity is strongly associated with the occurrence rate of CJs. As shown in Figure 3, the stars in our sample with multiple transiting SEs do have a slightly higher mean metallicity than those with a single transiting SE, but only by 0.03–0.04 dex. If the occurrence of CJs scales as $10^{2[\text{Fe}/\text{H}]}$ (Fischer & Valenti 2005), the difference in metallicity would lead to a difference of $\lesssim 20\%$ in the occurrence rates of CJs. This is too small to explain the observed contrast of $\gtrsim 500\%$.

7.4. Do Some of Single-transiting SE Systems Have Undetected Transiting SEs?

The stars we have classified as transit singles could really be multi-transiting systems for which some of the transiting planets were not detected due to a low signal-to-noise ratio. This would cloud any distinction between transit singles and multis. Specifically, this effect would increase the apparent fraction of stars with transit singles relative to transit multis and could result in a lower apparent occurrence of transiting CJs around

transit singles. If half of the observed transit singles are actually transit multis, for example, the numbers of stars with transit singles and multis in our sample reverse, and the inferred occurrence rates of transiting CJs among them would become less different. This is an issue for any comparison between transit singles and multis. Note, though, that here we are referring only to *transiting* planets that were missed, not about the planets that exist but do not transit.

To fully resolve this problem, we would need to observe the stars with a lower noise level, which is impractical. Nevertheless, we can place an empirical upper limit on the size of the problem. We wish to evaluate the probability \mathcal{P} that an observed transit single is actually a part of a transit multi:

$$\begin{aligned}
 \mathcal{P} &\equiv p(\text{true transit multi} | \text{obs. transit single}) \\
 &= \frac{p(\text{true transit multi})}{p(\text{obs. transit single})} \\
 &\quad \times p(\text{obs. transit single} | \text{true transit multi}) \\
 &= \frac{p(\text{obs. transit multi})}{p(\text{obs. transit single})} \\
 &\quad \times \frac{p(\text{obs. transit single} | \text{true transit multi})}{p(\text{obs. transit multi} | \text{true transit multi})}. \quad (7)
 \end{aligned}$$

Here “true” refers to the actual (but unknown) transit multiplicity, including the transiting planets that have not been detected; and “obs.” refers to the observed transit multiplicity, i.e., based on the number of detected transiting planets. In the last equality, we used the fact that the observed transit multis are subsets of true transit multis, i.e., $p(\text{obs. transit multi} | \text{true transit multi})$ equals $p(\text{obs. transit multi})/p(\text{true transit multi})$.

We need to evaluate the last term in Equation 7, which is the branching ratio for a true transit multi to be misclassified as a transit single: we will denote this ratio as $\mathcal{R}(\text{true transit multi})$. Although we do not know the architecture of true transit multis, we can place an em-

pirical limit on \mathcal{R} based on the *observed* sample of transit multis. The *observed* transit multis are no less likely to be observed as transit singles than true transit multis, because the observed transit multiplicity is always no more than the true transit multiplicity. Symbolically, $\mathcal{R}(\text{true transit multi}) \leq \mathcal{R}(\text{obs. transit multi})$.⁶ In this way, we can obtain an upper limit on \mathcal{R} using only the observed transit singles and multis.

We evaluate $\mathcal{R}(\text{obs. transit multi})$ by randomly assigning planets in the observed transit multis to stars hosting transit singles, and by counting how many of them would have been recovered by the *Kepler* transit-finding pipeline based on the transit signal to noise, following the procedure of [Fulton et al. \(2017\)](#). Based on 1,000 Monte Carlo realizations, we found $\mathcal{R}(\text{obs. transit multi}) = (19 \pm 2)\%$ and $\mathcal{P} \leq (11 \pm 1)\%$ for the confirmed SE sample, and $\mathcal{R}(\text{obs. transit multi}) = (22 \pm 2)\%$ and $\mathcal{P} \leq (8 \pm 1)\%$ for the candidate SE sample. The more stringent limit on \mathcal{P} for candidates is due to the larger fraction of transit singles in the candidate sample (71%) than in the confirmed sample (62%). We conclude that the sample of transit singles contains fewer than 10% of transit multis masquerading as transit singles. This difference is at most comparable to the difference in the fraction of transit singles between our confirmed and candidate SE samples, which yielded consistent results. Thus, the potential misclassification of transit multis as transit singles is unlikely to introduce a major bias in our inference. The same is likely true for other comparisons between transit singles and multis.

7.5. What About Stars with Multiple CJs?

The occurrence rate for CJs that we adopted for our analysis does not fully take into account the possible multiplicity of CJs. Indeed, among the 12 Doppler SE systems with CJs in the sample of [Zhu & Wu \(2018\)](#), four of them have two CJs with outer periods ranging from 2000 to 6000 days. [Zhu & Wu \(2018\)](#) derived the fraction of SE systems with at least one CJ, while [Bryan et al. \(2019\)](#) included only the innermost CJ to derive the occurrence. We used their results to calculate the probability to find one or zero transiting CJs in our sam-

⁶ Strictly speaking, systems with lower transit multiplicity could lead to lower \mathcal{R} than those with higher transit multiplicity if we consider the case where *all* the transiting planets are missed in a system. For example, if either zero or two transiting planets are always missed, for true transit doubles $\mathcal{R} = 0$, while for true transit triples $\mathcal{R} > 0$. However, our simulations using observed transit multis verify that such cases are rare: we find that \mathcal{R} does decrease with increasing transit multiplicity, as naively expected.

ple, because no star in our sample has more than one transiting CJ.

Our justification for this procedure is that even if multiple CJs exist, the innermost CJ is the most important one for our analysis, because it has a higher transit probability. Based on the CJ multiplicity observed by [Zhu & Wu \(2018\)](#), let us assume that 1/3 of our modeled CJ population with typical orbital periods of 1000 days (cf. Equation 5) also have outer CJs with typical periods of 3000 days (the geometric mean of the detected outer CJs in the sample). Then, taking into account both the geometric transit probability and the reduction factor of $4\text{yr}/P$ due to the finite duration of the prime *Kepler* mission, the fractional contribution to the total number of transiting CJs due to the outer planets would be on the order of $(1/3)/5 \sim 10\%$, a level of systematic error which is itself smaller than the uncertainty in the overall CJ occurrence.

In this light, our decision to consider only the inner CJs appears to be justified. Still, it is interesting to think about the sign of the possible bias. What happens if two CJs exist in reality? The rigorous answer depends on the period of the outer CJ and the mutual inclination between the two CJs, for which we have little or no information. If the two CJs have a high mutual inclination, the probability to observe at least one transiting CJ becomes larger than would be estimated by ignoring the outer CJ. This is because the orbital planes of the two CJs sweep out a larger area of the celestial sphere surrounding the star. In this case, the true mutual inclination dispersion between the SE and CJ would be larger than we have inferred. If, instead, the orbits of the two CJs are aligned, then the inner CJ is always more likely to transit, and the probability to find at least one transiting CJ is unchanged by the existence of the outer CJ.

7.6. Dilution due to Unresolved Companions

The *Kepler* transit signals were constructed by summing the light within a small collection of pixels surrounding the intended target star. Whenever this collection of pixels includes an unresolved star (whether a true companion, or a background object), the transit signal appears to be smaller because of the constant light from the neighboring object. The radii of planets in the same system could all be underestimated by a common factor if this “transit dilution” is not recognized.

This raises some questions regarding the purity and completeness of our sample. One question is whether some of the planets we have classified as inner SEs are actually giant planets. This is probably not a serious problem, because planets larger than $4 R_{\oplus}$ are intrinsi-

cally much rarer than smaller planets, when considering orbital periods shorter than 1 year. Another question is whether we have missed some SE systems because the transit signals have been diluted out of detectability. Most of the time, this type of error would not result in any bias in $n_{\text{tCJ}}(\mathcal{S})$ because the reason for their exclusion is independent of whether or not a transiting CJ is detected. The only problematic cases would be those for which there is enough dilution for an outer cold Jupiter to appear to have radii smaller than $7.5 R_{\oplus}$, but not so much dilution that the inner SEs would be rendered undetectable.

We think that such cases are rare enough to be negligible for our study, for two reasons. First, the required range of dilution factors (and hence the fraction of companions) that meet the conditions described above is quite limited. Let us consider the systems in Table 2 for which the outer planet appears to be too small to qualify as a CJ; could these outer planets really be giant planets for which the transit signal has been diluted? For KIC 5351250 and 7040629, this is unlikely. The radii would need to be underestimated by a factor of 3, which would imply that the compact inner systems consists of 3 or more planets with $r \gtrsim 4 R_{\oplus}$ — and such systems must be rare because only Kepler-51 (Steffen et al. 2013; Masuda 2014) and Kepler-31 (Fabrycky et al. 2012; Rowe et al. 2014) have such planets in the prime mission sample.⁷ For the other four stars (KIC 10187159, 8636333, 8738735, 10525077), the inner planets have 2–3 R_{\oplus} and would still qualify as SEs even if their radii are actually 1.3–2 times larger than they appear, in which case outer planets would be classified as CJs. This scenario requires that the transit depths be diluted by a factor of 1.7–4, and therefore that the flux of the unresolved object be 0.7–3 times that of the planet-hosting star. Assuming that the companion is physically bound and the luminosity scales as $\sim M_{\star}^4$ for main-sequence stars, this translates into a mass ratio of 0.9–1.3: the two stars need to be nearly twins. Considering the binary fraction of Sun-like stars and mass ratio distribution, only $\approx 20\%$ of stars might have such a companion, and in almost all cases it would have been noticed based on a double-lined spectrum or a luminosity that appears too high. Such coincidences would be even rarer for the case of an unrelated background star.

A second and more subtle reason is that when the determination of the stellar radius is based on the parallax, effective temperature, and apparent magnitudes, the estimated planetary radii are robust to errors due to dilu-

tion, especially for the case of twin binaries. The planetary radii are based on the observed transit depth δ , and the stellar radius is based on the *Gaia* parallax ϖ , effective temperature T_{eff} , and observed flux $F_{\star} \propto R_{\star}^2 \varpi^2 T_{\text{eff}}^4$. Thus the inferred planetary radius is $\propto \sqrt{\delta F_{\star}} / (\varpi T_{\text{eff}}^2)$. The combination δF_{\star} represents the *absolute* loss of flux during transits, i.e., the deficit in the number of photons. It does not depend on how many sources are contributing to the photometric signal. Another way to put it is that an unresolved companion causes the drop in relative flux to appear smaller, but also makes the host star appear brighter and larger. These two effects cancel out as long as the transit depth and stellar flux are measured in the same bandpass (which is true of *Kepler* and *Gaia*), and the measurement of the effective temperature is not significantly biased by the presence of the unresolved companion (which is true when the effective temperature is based on spectroscopy, or when the stars are nearly twins).

8. COMPARISON WITH Herman et al. (2019)

Herman et al. (2019) recently presented the results of an independent effort to determine mutual inclinations between the inner and outer parts of planetary systems. While our approach is based on counting transiting outer planets around stars with transiting inner planets, they took the opposite approach: counting the cases of transiting inner planets around stars with transiting outer planets. They performed the search for long-period transiting planets around Sun-like stars observed by *Kepler* using the automated pipeline by Foreman-Mackey et al. (2016), with refined stellar parameters from *Gaia* DR 2 and their own detrending of the light curves. Their sample includes 13 stars with long-period giant planets, of which five also have inner transiting systems consisting of SEs. Herman et al. (2019) pointed out that this relatively high occurrence of transiting SEs around stars with transiting CJs is consistent with a picture in which almost all long-period giant planets are associated with inner compact systems of smaller planets, with a typical mutual inclination of 4° between the inner and outer systems. Our analysis led to the inference of a somewhat higher mutual inclination of $11.8_{-5.5}^{+12.7}$ degrees. But it is difficult to make a rigorous comparison between the two analyses, for several reasons.

First, the sample of “cold giants” considered by Herman et al. (2019) includes planets as small as Neptune, for which the available Doppler data are insufficient to determine the conditional probability of occurrence around stars with inner SEs. This makes the conditional occurrence rate of SEs interior to their “cold gi-

⁷ Another such example has been recently reported around V1298 Tau from the *K2* sample (David et al. 2019).

ants” more uncertain than that for outer planets that meet our definition of “cold Jupiters.”

Second, their more inclusive definition of cold giants makes the sample more sensitive to selection effects. If the KOI stars have been searched more completely for transiting cold giants than the non-KOI stars (as one might expect, given that the data for KOI stars have lower noise, on average), the occurrence of transiting cold giants with inner planets (i.e., KOIs) would be overestimated, and the mutual orbital inclination would be underestimated. Indeed, if we select the sample using the same criteria but from the catalog of Kawahara & Masuda (2019), we find six stars with inner transiting planets among a total sample size of 27 transiting “cold giants.” The difference in the number of long-period giant planets arises because of the planets that were not detected by Herman et al. (2019). The resulting fraction $6/27 = 0.22$ is lower than the fraction $5/13 = 0.38$ adopted by Herman et al. (2019), and this increases the mutual inclination roughly by a factor of two.

Third, the fraction of transiting cold giants with inner transiting systems might be systematically affected by the multiplicity of the inner system, a possibility which was not taken into account in their analysis. As we noted in Section 7.5, this caveat also applies to our procedure for assigning CJs, but in their case the issue could be more serious because close-in SEs generally have higher multiplicity and smaller orbit spacings than CJs. There is also some evidence that compact multiple-planet systems occasionally have large mutual inclinations (Zhu et al. 2018). In general, any departure from perfectly-aligned orbits acts to increase the probability for *at least one* planet to transit, so ignoring this effect could lead to an underestimate of the typical mutual inclination.

Bearing all these difficulties in mind, we nevertheless tried applying our methodology to the sample of stars with transiting cold giants, adopting the assumption in Herman et al. (2019) that all the “cold giants” have inner SEs. We assigned one inner SE to each star with a period drawn randomly from the broken power-law distribution inferred for the entire *Kepler* SEs (Petrigura et al. 2018). We checked whether the simulated inner SEs transit or not, and if they did transit, we assumed the transit signals would always be detected. We adopted the same model for the mutual inclination distribution as in Equation 3, after swapping I_{SE} and I_{CJ} and setting I_{CJ} equal to 90° . For the 13 stars discussed by Herman et al. (2019), we found that five detections imply $\sigma = 5.0^{+3.4}_{-1.8}$ deg with 68% confidence, and $5.0^{+9.8}_{-2.9}$ deg with 95% confidence. When we performed the same exercise for the 27 stars identified by Kawahara & Masuda (2019), we found that six detections imply

$\sigma = 9.7^{+5.5}_{-2.9}$ deg with 68% confidence, and $9.7^{+15.7}_{-5.1}$ deg with 95% confidence. These inner systems include both single- and multi-transiting systems. Thus, we conclude that the number of transiting SEs found inside transiting long-period giants can be compatible with our analysis of the number of transiting cold Jupiters outside transiting SEs and the assumption that inner SEs exist around all stars with long-period planets of Neptune’s size or larger.

9. SUMMARY AND DISCUSSION

9.1. Overall Results

Among the sample of stars with close-orbiting super-Earths, there are too many cases of wide-orbiting transiting cold Jupiters for the orbital planes of the inner and outer systems to plausibly be uncorrelated. The enhancement in the number of outer transiting planets is about a factor of five for the entire sample of inner super-Earths, and a factor of 10 or more when the inner system has multiple transiting planets including super-Earths. Correspondingly, for the sample of stars with only one transiting super Earth, the number of detected transiting cold Jupiters is low enough to be compatible with uncorrelated orbital orientations.

We used these facts to derive constraints on the distribution of mutual inclinations between inner super-Earths and outer cold Jupiters. Specifically, we modeled the distribution as a von Mises–Fisher distribution and used the data to derive constraints on σ , the parameter specifying the width of the distribution.

As a whole, we found $\sigma = 11.8^{+12.7}_{-5.5}$ deg. Recalling that the CJs around stars with inner super-Earths can account for all the CJs uncovered from Doppler surveys, this implies that exoplanetary orbits in systems with CJs are in general dynamically hotter than the planetary orbits in the solar system (even though the solar system does have a “cold Jupiter”). This seems reasonable, given the broad eccentricity distribution of CJs that has been observed in Doppler surveys. Both the eccentricities and inclinations could be explained as the outcomes of planet–planet scattering in dynamically unstable systems of multiple giant planets (Chatterjee et al. 2008; Jurić & Tremaine 2008). Scattering simulations predict that the mean eccentricity and mean inclination should be of the same order of magnitude (see, e.g., Huang et al. 2017), and the inferred mean mutual inclination of our sample $(\pi/2)^{1/2}\sigma = 0.26$ rad is comparable to the mean eccentricity 0.3 of CJs.

We also found that a higher transit multiplicity of the inner system is associated with a lower mutual inclination relative to the cold Jupiter. For example, for inner systems having three or more transiting planets, we

found σ to be a few degrees, while for inner systems with only one transiting planet, we found $\sigma \gtrsim 20$ deg. Thus, the systems with well-aligned inner orbits are flat across the whole system (at the same level as in the Solar System), and were apparently unaffected by any dynamical disturbances after their formation. On the other hand, generic CJs have a broad range of eccentricities (and presumably a broad range of inclinations relative to the initial plane), and thus appear to be dynamically hotter than the undisturbed CJs around multi-transiting inner systems. This implies that the CJs with higher eccentricities (and inclinations) should generally be associated with inner systems with lower transit multiplicities, some of which are presumably dynamically hot systems with larger mutual inclinations as discussed in Section 1.

What could explain this association between the inner and outer systems, spanning an order of magnitude in orbital separation? It may be that the formation of dynamically hot outer systems facilitates the formation of dynamically hot inner systems, or vice versa. Alternatively, dynamical heating of both the inner and outer systems may result from a common cause, such as a difference in the protoplanetary disk or stellar environment. Below, we review some scenarios that have been proposed to explain the dynamically hot inner SE systems with low transit multiplicities, and we discuss how the association between the CJ–SE mutual inclination and inner transit multiplicity might also be explained in each scenario.

9.2. Relation to the Formation Scenarios of Dynamically Hot Systems of Super-Earths

9.2.1. Dynamical Heating Due to Outer CJs

The association between inner and outer systems can be explained if the inner system is dynamically heated due to gravitational perturbations from one or more mutually inclined cold Jupiters. It has been theoretically shown that secular perturbations can decrease the transit multiplicity of an inner system of super-Earths — either by eliminating some planets through ejections and collisions, or exciting mutual inclinations by driving differential nodal precession of the inner planetary orbits (Lai & Pu 2017; Huang et al. 2017; Gratia & Fabrycky 2017; Hansen 2017; Mustill et al. 2017; Pu & Lai 2018). In these scenarios, the first step is to raise the inclination (and eccentricity) of the outer planet due to interactions with other giant planets or a wider-orbiting companion star. Then, this dynamical excitation is spread to the inner system until the entire system is dynamically hot. The inner system may also be disrupted by direct interactions with outer giants (e.g., Huang et al. 2017; Mustill

et al. 2017). The cited works have demonstrated that such interactions often produce systems with mutual inclinations $> 10^\circ$, which are large enough to explain the distributions we have inferred.

The same type of scenario also naturally explains why the orbits of CJs are better aligned with the inner system when the inner system has multiple transiting planets. Even without violent interactions that would reduce the multiplicity of the inner system, an outer giant planet with a modest mutual inclination can disturb the coplanarity of the inner system. For example, Becker & Adams (2017) showed that typical *Kepler* systems with four or more transiting planets are easily perturbed out of multi-transiting configuration by CJs inside ~ 10 AU, unless the inner planets are strongly coupled with each other or the outer CJs are on well-aligned orbits. Such an architecture has been suggested for several multi-transiting systems with non-transiting CJs (e.g., Kepler-48, WASP-47; Lai & Pu 2017; Becker & Adams 2017; Read et al. 2017). Our result suggests that this is the case for general multi-transiting systems with outer CJs.

Hansen (2017) performed a population-level study of the effects of outer planets on inner multi-planetary systems. Prior simulations of the multi-planet systems based on the premise of *in situ* assembly (Hansen & Murray 2013) were able to match the observed properties of *Kepler* multis, but fell short in explaining the observed fraction of transit singles. Hansen (2017) found that the observed transit multiplicity function of the inner systems can be reproduced if about 40% of the *in situ* assembled inner systems were perturbed by dynamically excited outer giants with eccentricities and inclinations similar to the outcome of scattering simulations by Jurić & Tremaine (2008). The other $\approx 60\%$ of the systems remained unperturbed. The required CJ fraction is comparable to the observed rate from Doppler surveys, suggesting that excitation by outer planets could well be an important mechanism for sculpting the observed properties of the inner systems.⁸

9.2.2. Self-Excitation of the Inner System

Another proposal is that systems with lower transit multiplicities originate from “self-excitation”: dynamical heating due to planet–planet interactions among the SEs, rather than a wide-orbiting giant planet. Dawson et al. (2016) and Moriarty & Ballard (2016) stud-

⁸ Note, however, that in the simulation of Hansen (2017), the presence of multiple outer perturbers turned out to be important for efficiently heating the inner systems. The multiplicity of outer CJs is not yet observationally well constrained, and still needs to be investigated to test the validity of this model.

ied the excitation during the phase of *in situ* assembly and found that a diversity of dynamical states for compact multi-planet systems can arise from a corresponding diversity of surface density profiles and gas damping timescales in protoplanetary disks. While these models can also explain the observed transit multiplicity function,⁹ the excited inclinations in these models appear to be generally smaller (less than 10°) than the mutual inclination we inferred for CJs around transit singles and doubles. This is essentially because the eccentricity/inclination excitation for these close-in planets is limited by the strong influence of star’s gravity compared to the weak mutual gravitational interactions between low-mass planets. Similarly, it is difficult to excite $\gtrsim 10^\circ$ mutual inclinations via longer-term, secular self-excitation after the violent assembly through giant impacts is completed (Johansen et al. 2012; Becker & Adams 2016), because these processes do not produce sufficiently large mutual inclinations to explain the observed fraction of transit singles. Therefore, self-excitation within the inner SE system alone does not seem sufficient to explain the inferred mutual inclination distribution between SEs in low-transit-multiplicity systems and CJs. We note, though, that the conclusion depends on the unknown disk properties: for example, excitation of eccentricities and inclinations would be easier in more massive disks with shallower density profiles, in which outer planets have a larger angular momentum deficit that can be transferred to inner planets (Moriarty & Ballard 2016).

9.2.3. Summary of the Comparison

The preceding discussion suggests that the interactions between the inner and outer systems are essential to explain the inferred mutual inclinations. The facts that CJs are generally dynamically hot, and that most observed CJs are associated with inner SEs, also support the conclusion that there exist suitable initial configurations for outer planets to dynamically heat the inner system.

On the other hand, this does not necessarily exclude any contribution from self-excitation, or other possible mechanisms that can excite large mutual inclinations within the inner system. Indeed, the current data alone can also be compatible with a scenario in which the observed mutual CJ–SE inclinations simply scale with the mutual inclinations among the inner SE systems. The

model of intrinsic multiplicities and mutual inclinations of the compact *Kepler* systems by Zhu et al. (2018), as well as other “two population” models assuming the mixture of coplanar and mutually-inclined systems (Ballard & Johnson 2016; Mulders et al. 2018; He et al. 2019), suggest that the mutual inclination in the “dynamically hot” population could be as large as 10° or more. This value itself may be sufficient to explain the large CJ–SE mutual inclinations we inferred for transit singles (and doubles). Thus, models in which the excitation mechanism does not require CJs are still viable, as long as they can produce sufficiently large mutual inclinations in the inner systems ($\gtrsim 10^\circ$), and can explain the association between dynamically hot inner and outer systems. The latter would probably require a large-scale connection of the formation environments in the inner and outer region of the system — perhaps through a large-scale property of the protoplanetary disk.

Of course, the two scenarios are not mutually exclusive. Self-excitation can happen simultaneously in both inner and outer regions,¹⁰ and then the inner systems may further evolve under the gravitational influence of outer giants. Self-excitation might also facilitate such evolution, by producing inner systems with wider orbital spacings that are more easily disturbed by outer planets because of their weaker gravitational coupling.

The important difference between the two scenarios, though, is the expected dependence of CJ occurrence on the properties of the inner system. If the CJs are *causing* the inner system to be dynamically hot, then dynamically hot systems should always have CJs. This is not required in scenarios such as self-excitation. This leads us to adopt a working hypothesis that CJs are responsible for *all* the dynamically hot inner SE systems and explore its consequences and possible tests.

9.3. Could the CJs Play the Dominant Role?

If excitation by outer planets is the main way to form low-transit-multiplicity systems, we would expect the occurrence of CJs to be higher among stars with a smaller number of transiting SEs. This would invalidate an assumption we made in our analysis: we divided the sample based on inner transit multiplicity and assumed they all had the same rate of CJ occurrence. However, if CJs are actually more common around systems with lower transit multiplicities, this would only strengthen our conclusion that CJs around SE systems with lower transit multiplicities have higher mutual inclinations —

⁹ It should be noted, though, that Hansen & Murray (2013) could not reproduce the observed fraction of transit singles from their similar simulations, and the reason for this difference does not appear to be understood.

¹⁰ In principle, we do not need to distinguish the two regions. We have adopted this distinction because the region inside 1 AU is generally devoid of giant planets.

because we found fewer transiting CJs around such systems.

This scenario might appear to be contradicted by the lack of any clear difference in the $[\text{Fe}/\text{H}]$ distributions of stars with transit singles and transit multis (Weiss et al. 2018), as pointed out by Zhu et al. (2018). Because CJs occur more frequently around more metal-rich stars (e.g., Valenti & Fischer 2005), if stars with transit singles are preferentially associated with CJs, they would have relatively metal-rich hosts. However, the null result does not necessarily exclude an association between CJs and dynamically hot inner systems, considering that the population of transit singles consists of both dynamically hot systems and flatter multi-planet systems, with relative abundances that are not well constrained because of the degeneracy between intrinsic multiplicity and mutual inclination. In fact, Schlaufman (2014) argued that even if 50% of stars with SEs also have giant planets, the $[\text{Fe}/\text{H}]$ distribution of the host stars could still be statistically indistinguishable from a sample of SE host stars chosen randomly, without regard to outer giant planets.

We can flesh out this argument with the following construction. In the model of Zhu et al. (2018), the observed transit multiplicity distribution of *Kepler* systems may be explained if 25% of the systems belong to a dynamically hot population. Assume that all of these dynamically hot systems have CJs. Then, in order to produce an overall CJ occurrence of $1/3$ as observed, the CJ occurrence among the dynamically cold 75% of the sample needs to be $1/9$, viz., $1/3 = (1/4) \times 1 + (3/4) \times (1/9)$. Next, consider that $2/3$ of the *Kepler* systems are single-transiting systems. This implies that $(1/4)/(2/3) = 3/8$ of the transit singles are dynamically hot systems, and the other $5/8$ are dynamically cold. The CJ occurrence around transit singles is therefore $3/8 + (5/8) \times (1/9) = 4/9 = 44\%$. On the other hand, the CJ occurrence around transit multis, which are all dynamically cold, is only $1/9 = 11\%$. These values roughly agree with what has been observed in the available samples (Section 7.3). Also, the fraction of CJ hosts among transit singles (44%) is consistent with the current null detection of the difference in $[\text{Fe}/\text{H}]$ distribution, according to Schlaufman (2014).

Even if we should not expect any strong metallicity trends, we may still see some correlations arising from the association between the CJ occurrence and stellar metallicity. For example, the lack of high transit-multiplicity systems around metal-rich stars noted by Zhu & Wu (2018) could be due to the higher occurrence of CJs that reduce the transit multiplicity of the

inner system.¹¹ Similar correlations could be seen with any property that is correlated with the CJ occurrence, such as the stellar mass (Johnson et al. 2010). For example, the M-dwarf subsample of *Kepler* SEs appears to include a smaller fraction of transit singles (Moriarty & Ballard 2016) which could be connected to a lower CJ occurrence rate.

We note that the construction presented above is meant to show that the current data could be compatible with an (extreme) assumption that low-transit-multiplicity systems are entirely produced by external CJs. As we have discussed, the other extreme is that CJs are irrelevant, and the inferred CJ–SE mutual inclination simply mirrors the mutual inclinations of the inner SE system which were excited by other mechanisms. In this case, we would not expect any difference in CJ occurrence around systems with different transit multiplicities. This will be one of the key pieces of information to further shed light on the dominant mechanism to produce dynamically hot inner systems.

9.4. Future Probes

To summarize the overall story: compact systems of SEs exist around about $1/3$ of stars, of which $1/3$ also have CJs. The mutual inclinations between the orbits of the SEs and the CJs are generally on the order of 10° . Those systems that have larger inclinations tend to have lower transit multiplicities, hinting that the inner systems were dynamically heated by outer planets. There are several ways that the veracity of this story might be checked in the future.

Above all, we need more systems where both CJs and inner SEs can be detected and characterized. In particular, it is important to understand the dependence of CJ occurrence on the inner transit multiplicity to understand the role of CJs in shaping the system architecture. Such information may come from ongoing Doppler programs targeting *Kepler* systems (e.g., Mills et al. 2019b). Ultimately, *Gaia* data should also provide a large sample of stars which have both an inner system of transiting planets and an astrometrically-detected outer giant planets. The sample would also provide better and more direct constraints on the mutual inclination distribution, because the transit and astrometry data will constrain the line-of-sight inclinations of inner SEs and CJs, respectively.

It would also be of interest to compare the eccentricities of CJs outside transit singles and multis. If the

¹¹ Zhu & Wu (2018) interpreted this trend as the anti-correlation between CJs and the *intrinsic* multiplicity (rather than the transit multiplicity) of the inner system.

larger mutual inclinations around transit singles are indeed associated with dynamically hot CJs, rather than self-excited inner systems, we should see larger eccentricities for the CJs around transit singles as well — although this comparison may suffer from the same problem that we discussed in the previous section regarding the comparison of the [Fe/H] distributions. On the other hand, CJs around high transit multiplicity systems would generally have low eccentricities. The transit durations of the three CJs in our sample — all of which involve multi-transiting inner systems — are in fact consistent with low eccentricities (see Table 2), although the constraints are not very tight. Eccentricities may also be useful to test other possible mechanisms, such as star–planet interactions (Spalding & Batygin 2016) and warped disks (e.g., Zanazzi & Lai 2018), that can cause misalignments between the inner and outer system without violent dynamical excitation. If such mechanisms are significant, even inclined outer giants could still have circular orbits.

Measuring the obliquities of stars may also be useful as another way to identify the dynamically hot SE population. Although the $v \sin i$ distribution of transiting planet hosts does not show clear evidence that stars with transit singles and multis have different obliquity distributions (Hirano et al. 2014; Morton & Winn 2014; Winn et al. 2017), this may simply be due to the limited sensitivity of $v \sin i$ -based comparisons to small differences in inclination. In this regard, it is interesting that a highly oblique star with a single-transiting planet has been revealed by asteroseismology (Kamiaka et al. 2019). More precise measurements with the Rossiter–McLaughlin effects for a larger number of small transiting planets are warranted.

Although we focused exclusively on inner super-Earths smaller than $4 R_{\oplus}$ in this paper, some 50% of warm giants with 10 days $\lesssim P \lesssim 100$ days are known to co-exist with SEs in compact multi-planetary sys-

tems, possibly sharing a similar origin to the close-in SEs (Huang et al. 2016). Then, our inference might imply that similar misalignments also exist between warm giants and CJs. Such misalignments have been invoked theoretically to explain the population of eccentric warm Jupiters (Dong et al. 2014) and inferred observationally from the clustering of apsidal orientations of some warm- and cold-giant planet pairs on eccentric orbits (Dawson & Chiang 2014). This possibility may also be tested with the *Gaia* sample, and potentially has broader implications for the long-term dynamics of giant planets inside CJs. For example, misalignments are part of the initial conditions required to explain the large eccentricities of some warm giant planets (Anderson & Lai 2017). The excitation of large eccentricities, when combined with tidal dissipation, could also lead to the conversion of a warm giant into a hot Jupiter (Masuda 2017). A similar mechanism could also be responsible for the formation of hot sub-Neptunes and sub-Saturns, whose occurrence rates are correlated with stellar metallicity (Dong et al. 2018; Petigura et al. 2018), and hence the occurrence of CJs.

We thank Dan Foreman-Mackey for helpful conversations in the early stage of this work. We also thank an anonymous referee for careful reading of the manuscript and thoughtful suggestions on the interpretation of the results, which helped us to improve the manuscript. This paper includes data collected by the *Kepler* mission. Funding for the *Kepler* mission is provided by the NASA Science Mission directorate. This work was performed in part under contract with the California Institute of Technology (Caltech)/Jet Propulsion Laboratory (JPL) funded by NASA through the Sagan Fellowship Program executed by the NASA Exoplanet Science Institute. KM gratefully acknowledges the support by the W. M. Keck Foundation Fund.

REFERENCES

- Anderson, K. R., & Lai, D. 2017, *MNRAS*, 472, 3692, doi: [10.1093/mnras/stx2250](https://doi.org/10.1093/mnras/stx2250)
- Ballard, S., & Johnson, J. A. 2016, *ApJ*, 816, 66, doi: [10.3847/0004-637X/816/2/66](https://doi.org/10.3847/0004-637X/816/2/66)
- Becker, J. C., & Adams, F. C. 2016, *MNRAS*, 455, 2980, doi: [10.1093/mnras/stv2444](https://doi.org/10.1093/mnras/stv2444)
- . 2017, *MNRAS*, 468, 549, doi: [10.1093/mnras/stx461](https://doi.org/10.1093/mnras/stx461)
- Berger, T. A., Huber, D., Gaidos, E., & van Saders, J. L. 2018, *ApJ*, 866, 99, doi: [10.3847/1538-4357/aada83](https://doi.org/10.3847/1538-4357/aada83)
- Bryan, M. L., Knutson, H. A., Lee, E. J., et al. 2019, *AJ*, 157, 52, doi: [10.3847/1538-3881/aaf57f](https://doi.org/10.3847/1538-3881/aaf57f)
- Bryan, M. L., Knutson, H. A., Howard, A. W., et al. 2016, *ApJ*, 821, 89, doi: [10.3847/0004-637X/821/2/89](https://doi.org/10.3847/0004-637X/821/2/89)
- Butler, R. P., Wright, J. T., Marcy, G. W., et al. 2006, *ApJ*, 646, 505, doi: [10.1086/504701](https://doi.org/10.1086/504701)
- Chatterjee, S., Ford, E. B., Matsumura, S., & Rasio, F. A. 2008, *ApJ*, 686, 580, doi: [10.1086/590227](https://doi.org/10.1086/590227)
- Chiang, E., & Laughlin, G. 2013, *MNRAS*, 431, 3444, doi: [10.1093/mnras/stt424](https://doi.org/10.1093/mnras/stt424)

- Cui, X.-Q., Zhao, Y.-H., Chu, Y.-Q., et al. 2012, *Research in Astronomy and Astrophysics*, 12, 1197, doi: [10.1088/1674-4527/12/9/003](https://doi.org/10.1088/1674-4527/12/9/003)
- Cumming, A., Butler, R. P., Marcy, G. W., et al. 2008, *PASP*, 120, 531, doi: [10.1086/588487](https://doi.org/10.1086/588487)
- Dai, F., Masuda, K., & Winn, J. N. 2018, *ApJL*, 864, L38, doi: [10.3847/2041-8213/aadd4f](https://doi.org/10.3847/2041-8213/aadd4f)
- David, T. J., Petigura, E. A., Luger, R., et al. 2019, *ApJL*, 885, L12, doi: [10.3847/2041-8213/ab4c99](https://doi.org/10.3847/2041-8213/ab4c99)
- Dawson, R. I., & Chiang, E. 2014, *Science*, 346, 212, doi: [10.1126/science.1256943](https://doi.org/10.1126/science.1256943)
- Dawson, R. I., Lee, E. J., & Chiang, E. 2016, *ApJ*, 822, 54, doi: [10.3847/0004-637X/822/1/54](https://doi.org/10.3847/0004-637X/822/1/54)
- Dong, S., Katz, B., & Socrates, A. 2014, *ApJL*, 781, L5, doi: [10.1088/2041-8205/781/1/L5](https://doi.org/10.1088/2041-8205/781/1/L5)
- Dong, S., Xie, J.-W., Zhou, J.-L., Zheng, Z., & Luo, A. 2018, *Proceedings of the National Academy of Science*, 115, 266, doi: [10.1073/pnas.1711406115](https://doi.org/10.1073/pnas.1711406115)
- Eigmüller, P., Gandolfi, D., Persson, C. M., et al. 2017, *AJ*, 153, 130, doi: [10.3847/1538-3881/aa5d0b](https://doi.org/10.3847/1538-3881/aa5d0b)
- Fabrycky, D. C., Ford, E. B., Steffen, J. H., et al. 2012, *ApJ*, 750, 114, doi: [10.1088/0004-637X/750/2/114](https://doi.org/10.1088/0004-637X/750/2/114)
- Fabrycky, D. C., Lissauer, J. J., Ragozzine, D., et al. 2014, *ApJ*, 790, 146, doi: [10.1088/0004-637X/790/2/146](https://doi.org/10.1088/0004-637X/790/2/146)
- Fang, J., & Margot, J.-L. 2012, *ApJ*, 761, 92, doi: [10.1088/0004-637X/761/2/92](https://doi.org/10.1088/0004-637X/761/2/92)
- Fernandes, R. B., Mulders, G. D., Pascucci, I., Mordasini, C., & Emsenhuber, A. 2019, *ApJ*, 874, 81, doi: [10.3847/1538-4357/ab0300](https://doi.org/10.3847/1538-4357/ab0300)
- Figueira, P., Marmier, M., Boué, G., et al. 2012, *A&A*, 541, A139, doi: [10.1051/0004-6361/201219017](https://doi.org/10.1051/0004-6361/201219017)
- Fischer, D. A., & Valenti, J. 2005, *ApJ*, 622, 1102, doi: [10.1086/428383](https://doi.org/10.1086/428383)
- Fisher, R. A. 1953, *Proceedings of the Royal Society of London. Series A. Mathematical and Physical Sciences*, 217, 295, doi: [10.1098/rspa.1953.0064](https://doi.org/10.1098/rspa.1953.0064)
- Foreman-Mackey, D., Morton, T. D., Hogg, D. W., Agol, E., & Schölkopf, B. 2016, *AJ*, 152, 206, doi: [10.3847/0004-6256/152/6/206](https://doi.org/10.3847/0004-6256/152/6/206)
- Fulton, B. J., Petigura, E. A., Howard, A. W., et al. 2017, *AJ*, 154, 109, doi: [10.3847/1538-3881/aa80eb](https://doi.org/10.3847/1538-3881/aa80eb)
- Gaia Collaboration, Brown, A. G. A., Vallenari, A., et al. 2018, *A&A*, 616, A1, doi: [10.1051/0004-6361/201833051](https://doi.org/10.1051/0004-6361/201833051)
- Gratia, P., & Fabrycky, D. 2017, *MNRAS*, 464, 1709, doi: [10.1093/mnras/stw2180](https://doi.org/10.1093/mnras/stw2180)
- Grether, D., & Lineweaver, C. H. 2006, *ApJ*, 640, 1051, doi: [10.1086/500161](https://doi.org/10.1086/500161)
- Hansen, B. M. S. 2017, *MNRAS*, 467, 1531, doi: [10.1093/mnras/stx182](https://doi.org/10.1093/mnras/stx182)
- Hansen, B. M. S., & Murray, N. 2013, *ApJ*, 775, 53, doi: [10.1088/0004-637X/775/1/53](https://doi.org/10.1088/0004-637X/775/1/53)
- He, M. Y., Ford, E. B., & Ragozzine, D. 2019, *MNRAS*, 490, 4575, doi: [10.1093/mnras/stz2869](https://doi.org/10.1093/mnras/stz2869)
- Herman, M. K., Zhu, W., & Wu, Y. 2019, *AJ*, 157, 248, doi: [10.3847/1538-3881/ab1f70](https://doi.org/10.3847/1538-3881/ab1f70)
- Hirano, T., Sanchis-Ojeda, R., Takeda, Y., et al. 2014, *ApJ*, 783, 9, doi: [10.1088/0004-637X/783/1/9](https://doi.org/10.1088/0004-637X/783/1/9)
- Hirano, T., Narita, N., Sato, B., et al. 2012, *ApJL*, 759, L36, doi: [10.1088/2041-8205/759/2/L36](https://doi.org/10.1088/2041-8205/759/2/L36)
- Holman, M., Touma, J., & Tremaine, S. 1997, *Nature*, 386, 254, doi: [10.1038/386254a0](https://doi.org/10.1038/386254a0)
- Huang, C., Wu, Y., & TriAUD, A. H. M. J. 2016, *ApJ*, 825, 98, doi: [10.3847/0004-637X/825/2/98](https://doi.org/10.3847/0004-637X/825/2/98)
- Huang, C. X., Petrovich, C., & Deibert, E. 2017, *AJ*, 153, 210, doi: [10.3847/1538-3881/aa67fb](https://doi.org/10.3847/1538-3881/aa67fb)
- Izidoro, A., Raymond, S. N., Morbidelli, A., Hersant, F., & Pierens, A. 2015, *ApJL*, 800, L22, doi: [10.1088/2041-8205/800/2/L22](https://doi.org/10.1088/2041-8205/800/2/L22)
- Johansen, A., Davies, M. B., Church, R. P., & Holmelin, V. 2012, *ApJ*, 758, 39, doi: [10.1088/0004-637X/758/1/39](https://doi.org/10.1088/0004-637X/758/1/39)
- Johnson, J. A., Aller, K. M., Howard, A. W., & Crepp, J. R. 2010, *PASP*, 122, 905, doi: [10.1086/655775](https://doi.org/10.1086/655775)
- Johnson, J. A., Petigura, E. A., Fulton, B. J., et al. 2017, *AJ*, 154, 108, doi: [10.3847/1538-3881/aa80e7](https://doi.org/10.3847/1538-3881/aa80e7)
- Jurić, M., & Tremaine, S. 2008, *ApJ*, 686, 603, doi: [10.1086/590047](https://doi.org/10.1086/590047)
- Kamiaka, S., Benomar, O., Suto, Y., et al. 2019, *AJ*, 157, 137, doi: [10.3847/1538-3881/ab04a9](https://doi.org/10.3847/1538-3881/ab04a9)
- Kane, M., Ragozzine, D., Flowers, X., et al. 2019, *AJ*, 157, 171, doi: [10.3847/1538-3881/ab0d91](https://doi.org/10.3847/1538-3881/ab0d91)
- Kawahara, H., & Masuda, K. 2019, *AJ*, 157, 218, doi: [10.3847/1538-3881/ab18ab](https://doi.org/10.3847/1538-3881/ab18ab)
- Kipping, D. M. 2013, *MNRAS*, 434, L51, doi: [10.1093/mnras/slt075](https://doi.org/10.1093/mnras/slt075)
- Kipping, D. M., Torres, G., Henze, C., et al. 2016, *ApJ*, 820, 112, doi: [10.3847/0004-637X/820/2/112](https://doi.org/10.3847/0004-637X/820/2/112)
- Koch, D. G., Borucki, W. J., Basri, G., et al. 2010, *ApJL*, 713, L79, doi: [10.1088/2041-8205/713/2/L79](https://doi.org/10.1088/2041-8205/713/2/L79)
- Lai, D., & Pu, B. 2017, *AJ*, 153, 42, doi: [10.3847/1538-3881/153/1/42](https://doi.org/10.3847/1538-3881/153/1/42)
- Laughlin, G., Chambers, J., & Fischer, D. 2002, *ApJ*, 579, 455, doi: [10.1086/342746](https://doi.org/10.1086/342746)
- Lissauer, J. J., Ragozzine, D., Fabrycky, D. C., et al. 2011, *ApJS*, 197, 8, doi: [10.1088/0067-0049/197/1/8](https://doi.org/10.1088/0067-0049/197/1/8)
- Luo, A.-L., Zhao, Y.-H., Zhao, G., et al. 2015, *Research in Astronomy and Astrophysics*, 15, 1095, doi: [10.1088/1674-4527/15/8/002](https://doi.org/10.1088/1674-4527/15/8/002)
- Masuda, K. 2014, *ApJ*, 783, 53, doi: [10.1088/0004-637X/783/1/53](https://doi.org/10.1088/0004-637X/783/1/53)

- . 2017, *AJ*, 154, 64, doi: [10.3847/1538-3881/aa7aeb](https://doi.org/10.3847/1538-3881/aa7aeb)
- Mayor, M., Marmier, M., Lovis, C., et al. 2011, arXiv e-prints. <https://arxiv.org/abs/1109.2497>
- McArthur, B. E., Benedict, G. F., Barnes, R., et al. 2010, *ApJ*, 715, 1203, doi: [10.1088/0004-637X/715/2/1203](https://doi.org/10.1088/0004-637X/715/2/1203)
- Mills, S. M., & Fabrycky, D. C. 2017, *AJ*, 153, 45, doi: [10.3847/1538-3881/153/1/45](https://doi.org/10.3847/1538-3881/153/1/45)
- Mills, S. M., Howard, A. W., Petigura, E. A., et al. 2019a, *AJ*, 157, 198, doi: [10.3847/1538-3881/ab1009](https://doi.org/10.3847/1538-3881/ab1009)
- Mills, S. M., Howard, A. W., Weiss, L. M., et al. 2019b, *AJ*, 157, 145, doi: [10.3847/1538-3881/ab0899](https://doi.org/10.3847/1538-3881/ab0899)
- Moriarty, J., & Ballard, S. 2016, *ApJ*, 832, 34, doi: [10.3847/0004-637X/832/1/34](https://doi.org/10.3847/0004-637X/832/1/34)
- Morton, T. D., Bryson, S. T., Coughlin, J. L., et al. 2016, *ApJ*, 822, 86, doi: [10.3847/0004-637X/822/2/86](https://doi.org/10.3847/0004-637X/822/2/86)
- Morton, T. D., & Winn, J. N. 2014, *ApJ*, 796, 47, doi: [10.1088/0004-637X/796/1/47](https://doi.org/10.1088/0004-637X/796/1/47)
- Mulders, G. D., Pascucci, I., Apai, D., & Ciesla, F. J. 2018, *AJ*, 156, 24, doi: [10.3847/1538-3881/aac5ea](https://doi.org/10.3847/1538-3881/aac5ea)
- Mustill, A. J., Davies, M. B., & Johansen, A. 2017, *MNRAS*, 468, 3000, doi: [10.1093/mnras/stx693](https://doi.org/10.1093/mnras/stx693)
- Nesvorný, D., Kipping, D. M., Buchhave, L. A., et al. 2012, *Science*, 336, 1133, doi: [10.1126/science.1221141](https://doi.org/10.1126/science.1221141)
- Ormel, C. W., Liu, B., & Schoonenberg, D. 2017, *A&A*, 604, A1, doi: [10.1051/0004-6361/201730826](https://doi.org/10.1051/0004-6361/201730826)
- Petigura, E. A., Howard, A. W., Marcy, G. W., et al. 2017, *AJ*, 154, 107, doi: [10.3847/1538-3881/aa80de](https://doi.org/10.3847/1538-3881/aa80de)
- Petigura, E. A., Marcy, G. W., Winn, J. N., et al. 2018, *AJ*, 155, 89, doi: [10.3847/1538-3881/aaa54c](https://doi.org/10.3847/1538-3881/aaa54c)
- Pu, B., & Lai, D. 2018, *MNRAS*, 478, 197, doi: [10.1093/mnras/sty1098](https://doi.org/10.1093/mnras/sty1098)
- Ragozzine, D., & Holman, M. J. 2010, ArXiv e-prints. <https://arxiv.org/abs/1006.3727>
- Rasio, F. A., & Ford, E. B. 1996, *Science*, 274, 954, doi: [10.1126/science.274.5289.954](https://doi.org/10.1126/science.274.5289.954)
- Read, M. J., Wyatt, M. C., & Triaud, A. H. M. J. 2017, *MNRAS*, 469, 171, doi: [10.1093/mnras/stx798](https://doi.org/10.1093/mnras/stx798)
- Rowe, J. F., Bryson, S. T., Marcy, G. W., et al. 2014, *ApJ*, 784, 45, doi: [10.1088/0004-637X/784/1/45](https://doi.org/10.1088/0004-637X/784/1/45)
- Sanchis-Ojeda, R., Fabrycky, D. C., Winn, J. N., et al. 2012, *Nature*, 487, 449, doi: [10.1038/nature11301](https://doi.org/10.1038/nature11301)
- Schlaufman, K. C. 2014, *ApJ*, 790, 91, doi: [10.1088/0004-637X/790/2/91](https://doi.org/10.1088/0004-637X/790/2/91)
- Schmitt, J. R., Jenkins, J. M., & Fischer, D. A. 2017, *AJ*, 153, 180, doi: [10.3847/1538-3881/aa62ad](https://doi.org/10.3847/1538-3881/aa62ad)
- Spalding, C., & Batygin, K. 2016, *ApJ*, 830, 5, doi: [10.3847/0004-637X/830/1/5](https://doi.org/10.3847/0004-637X/830/1/5)
- Steffen, J. H., Fabrycky, D. C., Agol, E., et al. 2013, *MNRAS*, 428, 1077, doi: [10.1093/mnras/sts090](https://doi.org/10.1093/mnras/sts090)
- Thompson, S. E., Coughlin, J. L., Hoffman, K., et al. 2018, *ApJS*, 235, 38, doi: [10.3847/1538-4365/aab4f9](https://doi.org/10.3847/1538-4365/aab4f9)
- Tremaine, S., & Dong, S. 2012, *AJ*, 143, 94, doi: [10.1088/0004-6256/143/4/94](https://doi.org/10.1088/0004-6256/143/4/94)
- Uehara, S., Kawahara, H., Masuda, K., Yamada, S., & Aizawa, M. 2016, *ApJ*, 822, 2, doi: [10.3847/0004-637X/822/1/2](https://doi.org/10.3847/0004-637X/822/1/2)
- Valenti, J. A., & Fischer, D. A. 2005, *ApJS*, 159, 141, doi: [10.1086/430500](https://doi.org/10.1086/430500)
- Van Eylen, V., Albrecht, S., Huang, X., et al. 2019, *AJ*, 157, 61, doi: [10.3847/1538-3881/aaf22f](https://doi.org/10.3847/1538-3881/aaf22f)
- Wang, J., Fischer, D. A., Barclay, T., et al. 2015, *ApJ*, 815, 127, doi: [10.1088/0004-637X/815/2/127](https://doi.org/10.1088/0004-637X/815/2/127)
- Weidenschilling, S. J., & Marzari, F. 1996, *Nature*, 384, 619, doi: [10.1038/384619a0](https://doi.org/10.1038/384619a0)
- Weiss, L. M., Isaacson, H. T., Marcy, G. W., et al. 2018, *AJ*, 156, 254, doi: [10.3847/1538-3881/aae70a](https://doi.org/10.3847/1538-3881/aae70a)
- Winn, J. N., Petigura, E. A., Morton, T. D., et al. 2017, *AJ*, 154, 270, doi: [10.3847/1538-3881/aa93e3](https://doi.org/10.3847/1538-3881/aa93e3)
- Xie, J.-W., Dong, S., Zhu, Z., et al. 2016, *Proceedings of the National Academy of Science*, 113, 11431, doi: [10.1073/pnas.1604692113](https://doi.org/10.1073/pnas.1604692113)
- Zanazzi, J. J., & Lai, D. 2018, *MNRAS*, 477, 5207, doi: [10.1093/mnras/sty951](https://doi.org/10.1093/mnras/sty951)
- Zhu, W., Petrovich, C., Wu, Y., Dong, S., & Xie, J. 2018, *ApJ*, 860, 101, doi: [10.3847/1538-4357/aac6d5](https://doi.org/10.3847/1538-4357/aac6d5)
- Zhu, W., & Wu, Y. 2018, *AJ*, 156, 92, doi: [10.3847/1538-3881/aad22a](https://doi.org/10.3847/1538-3881/aad22a)
- Ziegler, C., Law, N. M., Baranec, C., et al. 2018, *AJ*, 156, 83, doi: [10.3847/1538-3881/aace59](https://doi.org/10.3847/1538-3881/aace59)